## Conflict of interest

The authors declare that they have no conflict of interest.

## References

Amano M, Nakayama M, Kaibuchi K (2010) Rho-kinase/ROCK: a key regulator of the cytoskeleton and cell polarity. *Cytoskeleton (Hoboken)* **67:** 545–554

Anagnostou VK, Syrigos KN, Bepler G, Homer RJ, Rimm DL (2009) Thyroid transcription factor 1 is an independent prognostic factor for patients with stage I lung adenocarcinoma. *J Clin Oncol* **27:** 271–278

Betapudi V, Licate LS, Egelhoff TT (2006) Distinct roles of non-muscle myosin II isoforms in the regulation of MDA-MB-231 breast cancer cell spreading and migration. *Cancer Res* **66:** 4725–4733

Bonne G, Carrier L, Bercovici J, Cruaud C, Richard P, Hainque B, Gautel M, Labeit S, James M, Beckmann J, Weissenbach J, Vosberg HP, Fiszman M, Komajda M, Schwartz K (1995) Cardiac myosin binding protein-C gene splice acceptor site mutation is associated with familial hypertrophic cardiomyopathy. *Nat Genet* **11:** 438–440

Chen CY, Schwartz RJ (1995) Identification of novel DNA binding targets and regulatory domains of a murine tinman homeodomain factor, nkx-2.5. *J Biol Chem* **270:** 15628–15633

Christiansen JJ, Rajasekaran AK (2006) Reassessing epithelial to mesenchymal transition as a prerequisite for carcinoma invasion and metastasis. *Cancer Res* **66:** 8319–8326

Conti MA, Adelstein RS (2008) Nonmuscle myosin II moves in new directions. *J Cell Sci* **121:** 11–18

Etienne-Manneville S, Hall A (2002) Rho GTPases in cell biology. *Nature* **420:** 629–635

Friedl P, Gilmour D (2009) Collective cell migration in morphogenesis, regeneration and cancer. *Nat Rev Mol Cell Biol* **10:** 445–457

Friedl P, Wolf K (2003) Tumour-cell invasion and migration: diversity and escape mechanisms. *Nat Rev Cancer* **3:** 362–374

Friedl P, Wolf K (2010) Plasticity of cell migration: a multiscale tuning model. *J Cell Biol* **188:** 11–19

Hall A (2009) The cytoskeleton and cancer. *Cancer Metastasis Rev* **28:** 5–14

Hidalgo-Carcedo C, Hooper S, Chaudhry SI, Williamson P, Harrington K, Leitinger B, Sahai E (2011) Collective cell migration requires suppression of actomyosin at cell-cell contacts mediated by DDR1 and the cell polarity regulators Par3 and Par6. *Nat Cell Biol* **13:** 49–58

Huang Y, Arora P, McCulloch CA, Vogel WF (2009) The collagen receptor DDR1 regulates cell spreading and motility by associating with myosin IIA. *J Cell Sci* **122:** 1637–1646

Itoh K, Yoshioka K, Akedo H, Uehata M, Ishizaki T, Narumiya S (1999) An essential part for Rho-associated kinase in the transcellular invasion of tumor cells. *Nat Med* **5:** 221–225

Kendall J, Liu Q, Bakleh A, Krasnitz A, Nguyen KC, Lakshmi B, Gerald WL, Powers S, Mu D (2007) Oncogenic cooperation and coamplification of developmental transcription factor genes in lung cancer. *Proc Natl Acad Sci USA* **104:** 16663–16668

Kimura S, Hara Y, Pineau T, Fernandez-Salguero P, Fox CH, Ward JM, Gonzalez FJ (1996) The T/ebp null mouse: thyroid-specific enhancer-binding protein is essential for the organogenesis of the thyroid, lung, ventral forebrain, and pituitary. *Genes Dev* **10:** 60–69

Kozaki K, Miyaishi O, Tsukamoto T, Tatematsu Y, Hida T, Takahashi T (2000) Establishment and characterization of a human lung cancer cell line NCI-H460-LNM35 with consistent lymphogenous metastasis via both subcutaneous and orthotopic propagation. *Cancer Res* **60:** 2535–2540

Kwei KA, Kim YH, Girard L, Kao J, Pacyna-Gengelbach M, Salari K, Lee J, Choi YL, Sato M, Wang P, Hernandez-Boussard T, Gazdar AF, Petersen I, Minna JD, Pollack JR (2008) Genomic profiling identifies TITF1 as a lineage-specific oncogene amplified in lung cancer. *Oncogene* **27:** 3635–3640

Lauffenburger DA, Horwitz AF (1996) Cell migration: a physically integrated molecular process. *Cell* **84:** 359–369

Li J, Gao E, Seidner SR, Mendelson CR (1998) Differential regulation of baboon SP-A1 and SP-A2 genes: structural and functional analysis of 5′-flanking DNA. *Am J Physiol* **275:** L1078–L1088

Maekawa M, Ishizaki T, Boku S, Watanabe N, Fujita A, Iwamatsu A, Obinata T, Ohashi K, Mizuno K, Narumiya S (1999) Signaling from Rho to the actin cytoskeleton through protein kinases ROCK and LIM-kinase. *Science* **285:** 895–898

Masuda A, Kondo M, Saito T, Yatabe Y, Kobayashi T, Okamoto M, Suyama M, Takahashi T (1997) Establishment of human peripheral lung epithelial cell lines (HPL1) retaining differentiated characteristics and responsiveness to epidermal growth factor, hepatocyte growth factor, and transforming growth factor beta1. *Cancer Res* **57:** 4898–4904

Matsumura F (2005) Regulation of myosin II during cytokinesis in higher eukaryotes. *Trends Cell Biol* **15:** 371–377

Medjkane S, Perez-Sanchez C, Gaggioli C, Sahai E, Treisman R (2009) Myocardin-related transcription factors and SRF are required for cytoskeletal dynamics and experimental metastasis. *Nat Cell Biol* **11:** 257–268

Pogach MS, Cao Y, Millien G, Ramirez MI, Williams MC (2007) Key developmental regulators change during hyperoxia-induced injury and recovery in adult mouse lung. *J Cell Biochem* **100:** 1415–1429

Richard P, Charron P, Carrier L, Ledeuil C, Cheav T, Pichereau C, Benaiche A, Isnard R, Dubourg O, Burban M, Gueffet JP, Millaire A, Desnos M, Schwartz K, Hainque B, Komajda M (2003) Hypertrophic cardiomyopathy: distribution of disease genes, spectrum of mutations, and implications for a molecular diagnosis strategy. *Circulation* **107:** 2227–2232

Riento K, Guasch RM, Garg R, Jin B, Ridley AJ (2003) RhoE binds to ROCK I and inhibits downstream signaling. *Mol Cell Biol* **23:** 4219–4229

Riento K, Ridley AJ (2003) Rocks: multifunctional kinases in cell behaviour. *Nat Rev Mol Cell Biol* **4:** 446–456

Sahai E, Marshall CJ (2002) ROCK and Dia have opposing effects on adherens junctions downstream of Rho. *Nat Cell Biol* **4:** 408–415

Sahai E, Marshall CJ (2003) Differing modes of tumour cell invasion have distinct requirements for Rho/ROCK signalling and extracellular proteolysis. *Nat Cell Biol* **5:** 711–719

Shibue T, Weinberg RA (2009) Integrin beta1-focal adhesion kinase signaling directs the proliferation of metastatic cancer cells disseminated in the lungs. *Proc Natl Acad Sci USA* **106:** 10290–10295

Takeuchi T, Tomida S, Yatabe Y, Kosaka T, Osada H, Yanagisawa K, Mitsudomi T, Takahashi T (2006) Expression profile-defined classification of lung adenocarcinoma shows close relationship

- 35 -

with underlying major genetic changes and clinicopathologic behaviors. *J Clin Oncol* **24:** 1679–1688

Tanaka H, Yanagisawa K, Shinjo K, Taguchi A, Maeno K, Tomida S, Shimada Y, Osada H, Kosaka T, Matsubara H, Mitsudomi T, Sekido Y, Tanimoto M, Yatabe Y, Takahashi T (2007) Lineage-specific dependency of lung adenocarcinomas on the lung development regulator TTF-1. *Cancer Res* **67:** 6007–6011

Tomida S, Takeuchi T, Shimada Y, Arima C, Matsuo K, Mitsudomi T, Yatabe Y, Takahashi T (2009) Relapse-related molecular signature in lung adenocarcinomas identifies patients with dismal prognosis. *J Clin Oncol* **27:** 2793–2799

Vicente-Manzanares M, Ma X, Adelstein RS, Horwitz AR (2009) Non-muscle myosin II takes centre stage in cell adhesion and migration. *Nat Rev Mol Cell Biol* **10:** 778–790

Watkins H, Conner D, Thierfelder L, Jarcho JA, MacRae C, McKenna WJ, Maron BJ, Seidman JG, Seidman CE (1995) Mutations in the cardiac myosin binding protein-C gene on chromosome 11 cause familial hypertrophic cardiomyopathy. *Nat Genet* **11:** 434–437

Watts RG, Howard TH (1992) Evidence for a gelsolin-rich, labile F-actin pool in human polymorphonuclear leukocytes. *Cell Motil Cytoskeleton* **21:** 25–37

Weir BA, Woo MS, Getz G, Perner S, Ding L, Beroukhim R, Lin WM, Province MA, Kraja A, Johnson LA, Shah K, Sato M, Thomas RK, Barletta JA, Borecki IB, Broderick S, Chang AC, Chiang DY, Chirieac LR, Cho J *et al* (2007) Characterizing the cancer genome in lung adenocarcinoma. *Nature* **450:** 893–898

Welikson RE, Fischman DA (2002) The C-terminal IgI domains of myosin-binding proteins C and H (MyBP-C and MyBP-H) are both necessary and sufficient for the intracellular crosslinking of sarcomeric myosin in transfected non-muscle cells. *J Cell Sci* **115:** 3517–3526

White CW, Greene KE, Allen CB, Shannon JM (2001) Elevated expression of surfactant proteins in newborn rats during adaptation to hyperoxia. *Am J Respir Cell Mol Biol* **25:** 51–59

Wilkinson S, Paterson HF, Marshall CJ (2005) Cdc42-MRCK and Rho-ROCK signalling cooperate in myosin phosphorylation and cell invasion. *Nat Cell Biol* **7:** 255–261

Winslow MM, Dayton TL, Verhaak RG, Kim-Kiselak C, Snyder EL, Feldser DM, Hubbard DD, DuPage MJ, Whittaker CA, Hoersch S, Yoon S, Crowley D, Bronson RT, Chiang DY, Meyerson M, Jacks T (2011) Suppression of lung adenocarcinoma progression by Nkx2-1. *Nature* **473:** 101–104

Wong CC, Wong CM, Ko FC, Chan LK, Ching YP, Yam JW, Ng IO (2008) Deleted in liver cancer 1 (DLC1) negatively regulates Rho/ROCK/MLC pathway in hepatocellular carcinoma. *PLoS One* **3:** e2779

Yamamoto K (1988) Effect of H-protein on the formation of myosin filaments and light meromyosin paracrystals. *J Biochem* **103:** 274–280

Yatabe Y, Mitsudomi T, Takahashi T (2002) TTF-1 expression in pulmonary adenocarcinomas. *Am J Surg Pathol* **26:** 767–773

Yoneda A, Multhaupt HA, Couchman JR (2005) The Rho kinases I and II regulate different aspects of myosin II activity. *J Cell Biol* **170:** 443–453

Yoshioka K, Foletta V, Bernard O, Itoh K (2003) A role for LIM kinase in cancer invasion. *Proc Natl Acad Sci USA* **100:** 7247–7252

# NKX2-1/TITF1/TTF-1-Induced ROR1 Is Required to Sustain EGFR Survival Signaling in Lung Adenocarcinoma

Tomoya Yamaguchi,[1] Kiyoshi Yanagisawa,[1,2] Ryoji Sugiyama,[1] Yasuyuki Hosono,[1] Yukako Shimada,[1] Chinatsu Arima,[1] Seiichi Kato,[3] Shuta Tomida,[1] Motoshi Suzuki,[1] Hirotaka Osada,[4] and Takashi Takahashi[1,*]

[1]Division of Molecular Carcinogenesis, Center for Neurological Diseases and Cancer, Nagoya University Graduate School of Medicine, Showa-ku, Nagoya 466-8550, Japan
[2]Institute for Advanced Research, Nagoya University, Chikusa-ku, Nagoya 464-8601, Japan
[3]Department of Pathology and Laboratory Medicine, Nagoya University Hospital, Showa-ku, Nagoya 466-8550, Japan
[4]Division of Molecular Oncology, Aichi Cancer Center Research Institute, Chikusa-ku, Nagoya 464-8681, Japan
*Correspondence: tak@med.nagoya-u.ac.jp
DOI 10.1016/j.ccr.2012.02.008

## SUMMARY

We and others previously identified *NKX2-1*, also known as *TITF1* and *TTF-1*, as a lineage-survival oncogene in lung adenocarcinomas. Here we show that NKX2-1 induces the expression of the receptor tyrosine kinase-like orphan receptor 1 (*ROR1*), which in turn sustains a favorable balance between prosurvival PI3K-AKT and pro-apoptotic p38 signaling, in part through ROR1 kinase-dependent c-Src activation, as well as kinase activity-independent sustainment of the EGFR-ERBB3 association, ERBB3 phosphorylation, and consequential PI3K activation. Notably, ROR1 knockdown effectively inhibited lung adenocarcinoma cell lines, irrespective of their EGFR status, including those with resistance to the EGFR tyrosine kinase inhibitor gefitinib. Our findings thus identify ROR1 as an "Achilles' heel" in lung adenocarcinoma, warranting future development of therapeutic strategies for this devastating cancer.

## INTRODUCTION

It is well understood that oncogene addiction is present in certain cancers, with lung adenocarcinomas carrying epidermal growth factor receptor (EGFR) mutations among the best examples (Weinstein, 2002). Emerging evidence, though currently sparse, suggests that "lineage-specific transcription factors" with developmental roles in normal progenitor cells of particular lineages may also confer dependency for survival to certain types of cancer cells (Garraway and Sellers, 2006). The basic helix-loop-helix (bHLH) transcription factor MITF in melanoma has been proposed as an archetypal prototype. Along this line, our previous studies demonstrated that achaete-scute homolog 1 (ASH1)/achaete-scute complex-like 1, a bHLH protein indis-pensable for pulmonary neuroendocrine cell development, is also required for survival of lung cancers with neuroendocrine features, such as small cell lung cancers (Nishikawa et al., 2011; Osada et al., 2005, 2008).

Lung cancer is the leading cause of cancer death, whereas adenocarcinomas arising from peripheral lung are the most frequent histological type and exhibit the highest degree of heterogeneity. NKX2-1, a homeodomain transcription factor also known as TITF1 and TTF-1, plays an essential role in peripheral lung development, and NKX2-1 deficiency in mice results in lung aplasia (Kimura et al., 1996). We previously reported that NKX2-1 is a reliable lineage marker for terminal respiratory unit (TRU) cells, as well as for "TRU-type" adenocarcinomas with distinct gene expression profiles, which show abundant

---

### Significance

NKX2-1-induced ROR1 is required to sustain a favorable balance between prosurvival PI3K-AKT signaling and the pro-apoptotic p38 pathway, the collapse of which elicits "oncogenic shock." ROR1 was also identified as a receptor tyrosine kinase with a "sustainer role" for the EGFR-ERBB3-mediated signaling. Mechanisms, such as a secondary EGFR mutation, MET amplification, and HGF overexpression, may arise in lung adenocarcinomas of patients undergoing EGFR-TKI treatment and lead to tumor resistance of the treatment. Such diverse mechanisms make it difficult to predict which should be targeted to prevent expansion of resistant clones. From a clinical point of view, it is thus of particular interest that ROR1 inhibition appears to be effective in treatment of gefitinib-resistant lung adenocarcinomas with various resistance mechanisms.
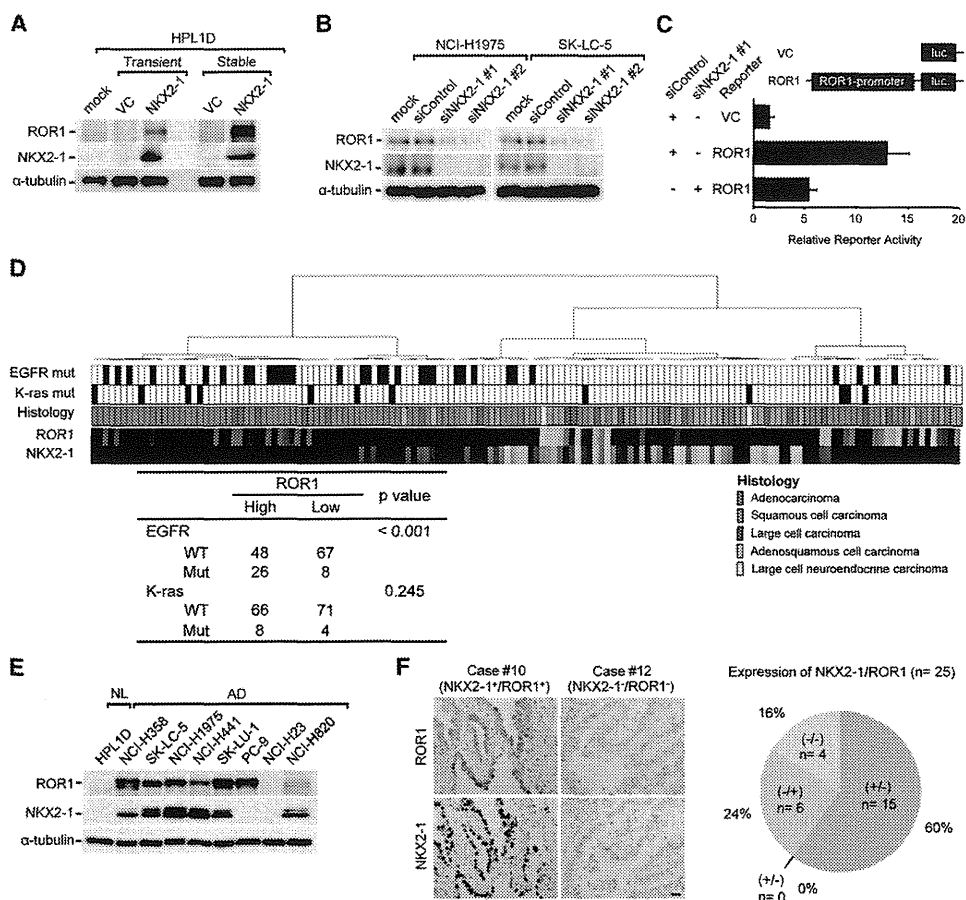
**Figure 1. *ROR1* Is Transactivated by NKX2-1**

(A) WB analysis of NKX2-1-transfected HPL1D.

(B) WB analysis of siNKX2-1-introduced NKX2-1⁺/ROR1⁺ lung adenocarcinoma cell lines. siControl, negative control siRNA; siNKX2-1 #1 and #2, siRNAs against NKX2-1.

(C) Luciferase reporter assay of ROR1 promoter showing reduced activity in response to NKX2-1 silencing in a stable NKX2-1 transfectant of HPL1D. Data are shown as the mean ± SD (n = 3).

(D) Hierarchical clustering analysis of non-small-cell lung cancers using a microarray dataset along with information regarding the relationship of *ROR1* expression with *EGFR* and *K-ras* mutations.

(E) Western blot analysis of ROR1 and NKX2-1 in lung adenocarcinoma and normal lung epithelial cell lines. NL, normal lung; AD, lung adenocarcinoma.

(F) Representative ROR1 staining in lung adenocarcinoma specimens and a summary of immunohistochemical analysis (n = 25). Scale bar, 100 μm. See also Figure S1 and Table S1.

*NKX2-1* expression, as well as characteristic clinicopathologic and genetic features, including a significant association with *EGFR* mutations (Takeuchi et al., 2006; Yatabe et al., 2002, 2005). We further identified NKX2-1 as a lineage-survival oncogene in lung adenocarcinoma (Tanaka et al., 2007); other investigators reached similar conclusions through genome-wide searches for focal genomic aberrations (Kendall et al., 2007; Kwei et al., 2008; Weir et al., 2007).

Previous findings, including ours, thus clearly indicate the requirement of sustained NKX2-1 expression for lung adenocarcinoma survival, though how NKX2-1 mediates survival signals remains elusive. It should be noted that NKX2-1 itself is well known to play indispensable roles in the maintenance of normal lung physiology, such as transcriptional activation of surfactant protein genes (Boggaram, 2009). In the present study, we therefore aimed to elucidate downstream signaling by NKX2-1, since

such understanding appears to be a crucial step in the development of a therapeutic strategy for targeting NKX2-1-mediated survival signaling.

## RESULTS

### Identification of ROR1 as a Direct Transcriptional Target for NKX2-1

To better understand how NKX2-1 mediates survival signals in lung adenocarcinomas, we performed microarray analysis using HPL1D, an immortalized human peripheral lung epithelial cell line (Masuda et al., 1997), which was stably introduced with NKX2-1. Consequently, *ROR1* was identified among the most highly upregulated genes (Figure S1A available online). NKX2-1-mediated ROR1 induction was validated by western blot analysis using NKX2-1 transfectants (Figure 1A), as well as
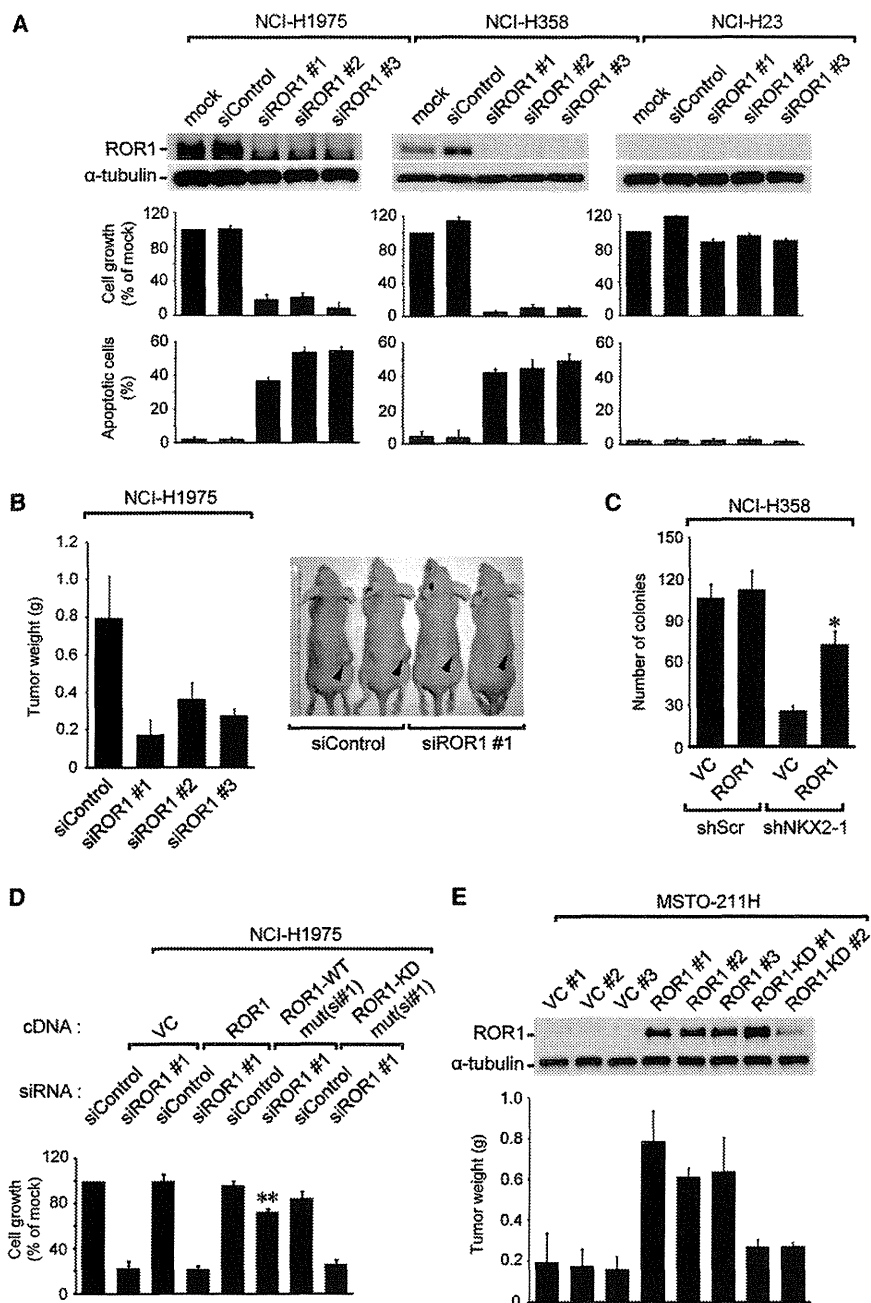
**Figure 2. ROR1 Sustains Lung Adenocarcinoma Survival**

(A) Assays for measuring the effects of ROR1 knockdown in growth inhibition and apoptosis induction in lung adenocarcinoma cell lines. siControl, negative control siRNA; siROR1 #1 to #3, siRNA against ROR1. Data are shown as the mean ± SD (n = 3).

(B) In vivo treatment of xenografts with ROR1 siRNA. Two weeks after intratumoral siRNA injection, photographs were obtained and tumor weights measured. Data are shown as the mean ± SD (n = 7).

(C) Alleviation of siNKX2-1-mediated growth inhibition by ROR1 introduction. Colonies were counted two weeks after cotransfection of the expression vectors of ROR1 and short hairpin RNA against NKX2-1 in NKX2-1$^+$/ROR1$^+$ NCI-H358. Data are shown as the mean ± SD (n = 3). *p < 0.05 versus VC+shNKX2-1, as determined by Student's t test.

(D) Colorimetric assays of cells treated with siROR1, along with wild-type ROR1 [ROR1-mut(si#1)] or kinase-dead ROR1 [ROR1-KD mut(si#1)], each with silent mutations at the siRNA binding site. Data are shown as the mean ± SD (n = 3). **p < 0.001 versus siROR1#1+ROR1, as determined by Student's t test.

(E) In vivo tumor growth assay in stable wild-type or kinase-dead ROR1 transfectants of MSTO-211H. Three weeks after subcutaneous inoculation, tumor weights were measured. Data are shown as the mean ± SD (n = 5). See also Figure S2.

lung adenocarcinoma cell lines treated with siRNA against NKX2-1 (siNKX2-1; Figure 1B). A luciferase reporter assay with the 1.0 kb human ROR1 promoter region showed its NKX2-1-dependent activation (Figure 1C), and a chromatin immunoprecipitation (ChIP) assay revealed direct binding of NKX2-1 to the ROR1 promoter (Figure S1B), demonstrating that *ROR1* is a direct transcriptional target for NKX2-1. Co-expression of *NKX2-1* and *ROR1* was preferentially observed in adenocarcinomas in analysis of our previous microarray dataset of 149 non-small lung cancer patients (Figure 1D; Takeuchi et al., 2006; GEO accession number: GSE11969), whereas the presence of *EGFR* mutations was found to be associated with a high expression of *ROR1*. A similar association between NKX2-1 and ROR1 expres-

sion was also confirmed at the protein level in panels of lung adenocarcinoma cell lines and tumor specimens (Figures 1E and 1F and Table S1). However, we also noted some instances of NKX2-1$^-$/ROR1$^+$, suggesting that the expression of ROR1 may be also regulated by other transcription factors.

**Involvement of ROR1 in NKX2-1-Mediated Survival Signaling in Lung Adenocarcinomas**

Next, we examined whether ROR1 knockdown affects survival in lung adenocarcinoma cells. siROR1 treatment was shown to induce significant growth inhibition of ROR1-positive lung adenocarcinoma cell lines in association with apoptosis induction, whereas ROR1-negative lung adenocarcinoma cell lines, as well as primary normal lung epithelial cells, did not show any growth inhibition (Figures 2A and S2A–S2C). In addition, intratumoral injection of ROR1 siRNAs with atelocollagen significantly reduced in vivo growth of NCI-H1975 xenografts (Figure 2B). We also investigated whether exogenously introduced ROR1 could mitigate NKX2-1-knockdown-induced growth inhibition. Forced ROR1 expression resulted in significant, though not complete, alleviation of growth inhibition imposed by the expression of short hairpin RNA against NKX2-1 in NKX2-1$^+$/ROR1$^+$ NCI-H358 cells,
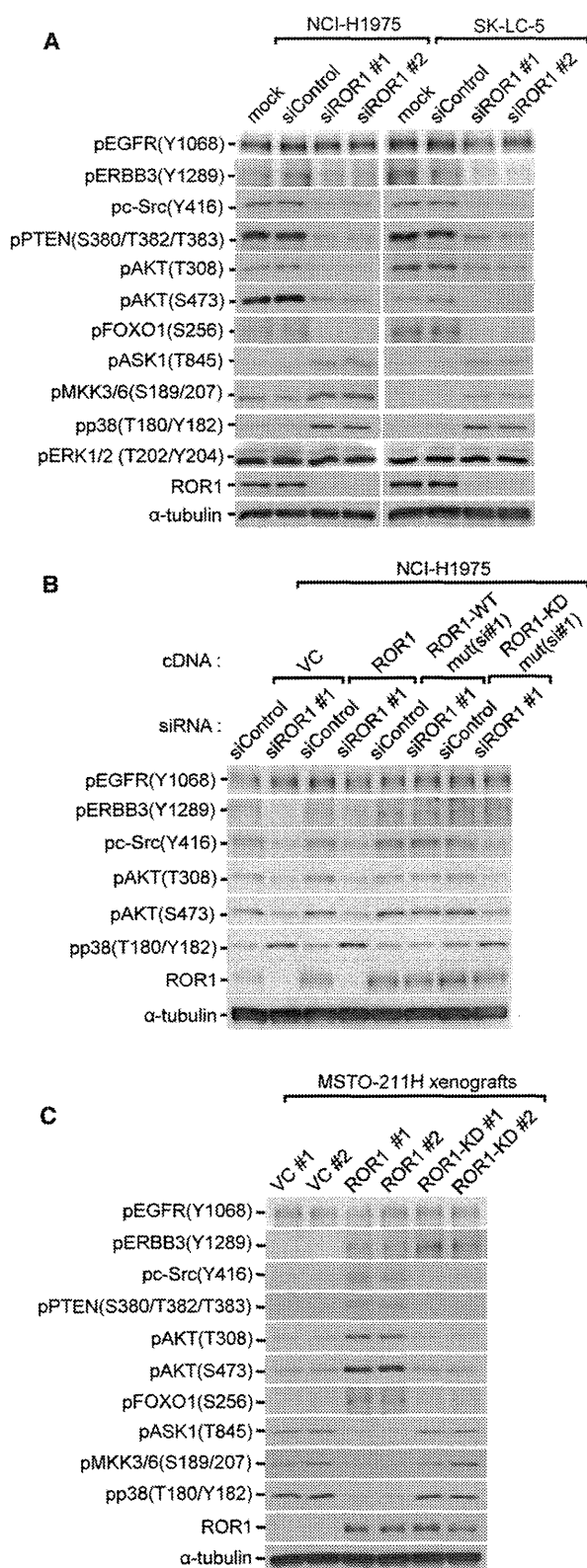
**A**



**B**



**C**



**Figure 3. ROR1 Affects Both PI3K-AKT Prosurvival and Pro-Apoptotic p38 Signaling**

(A) WB analysis of the prosurvival and pro-apoptotic signaling molecules in siROR1-treated adenocarcinoma cells.

supporting the notion that NKX2-1-induced survival signaling is conferred, at least in part, through induction of ROR1 (Figure 2C). Interestingly, we found that the wild-type but not kinase-dead ROR1 with silent mutations at the siRNA binding site was able to counteract siROR1-induced growth inhibition (Figure 2D). Concordantly, forced expression of wild-type ROR1 but not kinase-dead ROR1 in ROR1-negative MSTO-211H cells at a level comparable to that in NCI-H1975 cells enhanced in vivo growth of the xenografts (Figures 2E, S2D, and S2E), suggesting that ROR1 kinase activity is required to fully confer a growth advantage.

## Identification of ROR1-EGFR Interaction Sustaining EGFR-ERBB3-PI3K Signaling

We also examined how ROR1 mediates survival signals in lung adenocarcinomas. ROR1 knockdown decreased phosphorylations of ERBB3, c-Src, and AKT in NKX2-1[+]/ROR1^{+} NCI-H1975, SK-LC-5, and NCI-H358 cells (Figures 3A, S3A, and S3B). siROR1 treatment also reduced phosphorylation of FOXO1, downstream of AKT, whereas p38 phosphorylation was induced in siROR1-treated cells, in association with increased phosphorylations of its upstream kinases ASK1 and MKK3/6. In contrast, phosphorylations of EGFR and ERK1/2 were not affected by ROR1 knockdown. Introduction of exogenous wild-type ROR1 with silent mutations at the siRNA binding site cancelled effects on downstream signaling, demonstrating the specificity of siRNA-mediated ROR1 knockdown (Figure 3B). We noted that forced expression of kinase-dead ROR1 with the silent mutations restored ERBB3 phosphorylation, whereas it failed to mitigate siROR1-induced effects on c-Src, p38, and AKT phosphorylations (Figure 3B). Conversely, opposite effects on the phosphorylations of potential downstream molecules were observed in wild-type, but not kinase-dead, ROR1-introduced MSTO-211H xenografts, whereas increased ERBB3 phosphorylation was detected in both wild-type and kinase-dead ROR1-introduced xenografts (Figure 3C).

EGFR by itself is an efficient initiator of ERK through homo-dimer formation, though it is a poor activator of PI3K signaling (Sharma and Settleman, 2009). In addition, EGF-induced EGFR activation is linked to PI3K through phosphorylation of intrinsically kinase-deficient ERBB3 but not EGFR in lung adenocarcinoma cells (Engelman et al., 2005; Rothenberg et al., 2008). We found that ROR1 knockdown selectively diminished EGF treatment-induced ERBB3 phosphorylation without appreciably affecting the phosphorylation of EGFR itself in NCI-H1975 and SK-LC-5 cells (Figure 4A), which appeared to be consistent with the lack of effects seen with ROR1 knockdown on ERK phosphorylation. ROR1 knockdown also abrogated EGF-induced phosphorylation of AKT and FOXO1, whereas decreased c-Src phosphorylation and induction of p38 phosphorylation were elicited by siROR1 treatment regardless of the presence or absence of EGF. Marked nuclear retention, hence activation of apoptosis-inducing FOXO1, a target of the

(B) WB analysis of lung adenocarcinoma cells concurrently treated with siROR1 and RNAi-resistant wild-type ROR1 [ROR1-mut(si#1)] or kinase-dead ROR1 [ROR1-KD mut(si#1)].

(C) WB analysis of signaling molecules in ROR1 stable transfectants. ROR1-KD, kinase-dead ROR1. See also Figure S3.
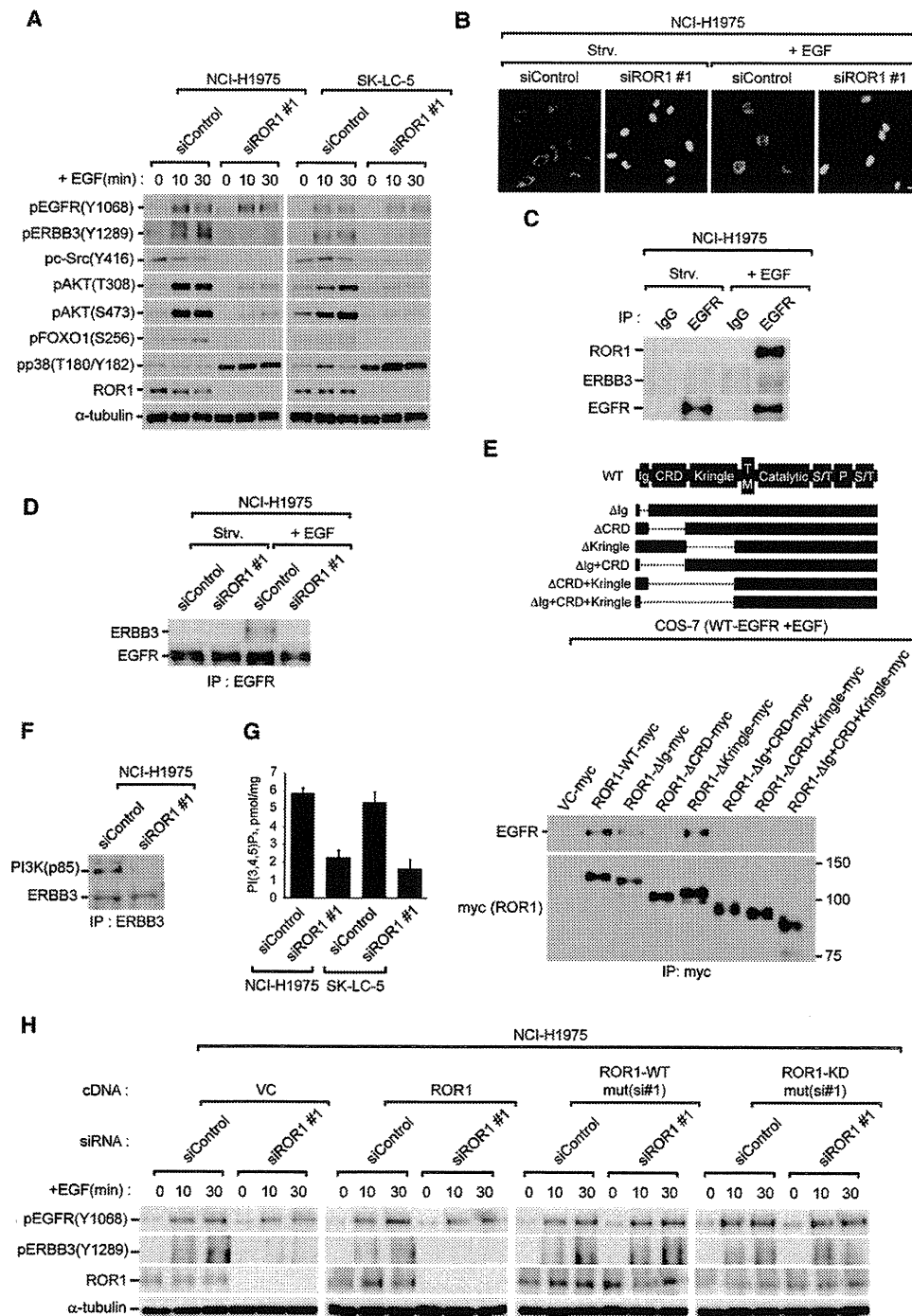
**Figure 4. ROR1 Sustains EGF-Induced Signaling through ERBB3**

(A) WB analysis of downstream molecules in EGF-treated and ROR1-silenced NCI-H1975 and SK-LC-5.

(B) Immunofluorescence staining of FOXO1 in ROR1-silenced NCI-H1975 in the presence or absence of EGF. Scale bar, 30 μm. Strv, serum starved.

(C) IP-WB analysis of EGF-stimulated association of EGFR with ROR1 or ERBB3 in NCI-H1975. Strv, serum starved.

(D) IP-WB analysis of EGFR-ERBB3 association in response to EGF, with and without siROR1 treatment, in NCI-H1975. Strv, serum starved.

(E) IP-WB analysis of ROR1-EGFR association in COS-7 cotransfected with EGFR and various ROR1 deletion mutants.

(F) IP-WB analysis of the interaction between ERBB3 and p85 (PI3K), with and without siROR1 treatment, in NCI-H1975.

(G) In vitro PI3K assay with immunoprecipitated PI3K from siROR1-treated NCI-H1975 or SK-LC-5 cell lysates. Data are shown as the mean ± SD (n = 3).

(H) WB analysis of EGF-induced EGFR and ERBB3 phosphorylation in the presence or absence of siROR1 treatment in siRNA-resistant wild-type [ROR1-mut(si#1)] or kinase-dead [ROR1-mut(si#1)] ROR1-introduced NCI-H1975 cells. See also Figure S4.

-41-

PI3K-AKT axis (Calnan and Brunet, 2008), was also observed in response to siROR1 treatment (Figure 4B). Interestingly, EGF treatment induced an association of ROR1 with EGFR in NCI-H1975 cells, as well as in COS-7 cells cotransfected with both ROR1 and EGFR (Figures 4C and S4A, respectively). Immuno-precipitation (IP)-western blot (WB) analysis also revealed that ROR1 knockdown significantly reduced co-immunoprecipitation of EGFR with ERBB3 in EGF-stimulated NCI-H1975 cells (Figure 4D). It was further shown that a cysteine-rich domain of the extracellular domain of ROR1 is required for association with EGFR (Figures 4E and S4B). In line with enhancement of EGF-induced ERBB3 phosphorylation by ROR1, its knockdown led to significantly reduced binding of the p85 subunit of PI3K to ERBB3 (Figure 4F). In addition, an in vitro PI3K assay using PI3K immunoprecipitated from siROR1-treated NCI-H1975 and SK-LC-5 cell lysates showed reduced conversion of $PIP_3$ (Figure 4G), demonstrating that ROR1 knockdown negatively affects PI3K activity. Interestingly, both wild-type and kinase-dead ROR1 with silent mutations at the siRNA binding site were able to restore EGF-induced ERBB3 phosphorylation in NCI-H1975 cells, indicating that ROR1 kinase activity is not indispensable in this regard (Figure 4H). Taken together, these findings indicated that ROR1 kinase activity is not indispensable for sustaining ROR1-EGFR interaction, EGFR-ERBB3 interaction, and ERBB3 phosphorylation, whereas ROR1 kinase activity is required to fully sustain downstream signaling and survival, suggesting the involvement of additional downstream signaling.

## Identification of c-Src as a Downstream Molecule in ROR1-Mediated Survival Signaling

We accordingly sought an additional, underlying mechanism by which ROR1 fully sustains survival signaling in lung adenocarcinomas. Contrasting changes in c-Src Y416 phosphorylation in response to altered ROR1 expression caught our attention, since it suggested a possible, functional relationship. We found that introduction of constitutively active c-Src noticeably alleviated ROR1-silencing-induced effects, including growth inhibition, and reduced phosphorylations of PTEN and AKT, both of which are known to be downstream of c-Src (Figure 5A; Hennessy et al., 2005; Martin, 2001). ROR1 knockdown-induced p38 phosphorylation was also clearly counteracted by the introduction of constitutively active c-Src. Of note, c-Src inactivation by either siRNAs or a c-Src inhibitor (SKI-1) had effects very similar to ROR1 knockdown in terms of both growth inhibition and signaling in ROR1-positive NCI-H1975 and SK-LC-5 cells (Figures 5B), whereas ROR1-negative NCI-H23 cells had virtually no response to c-Src inhibition (Figure S5A). IP-WB analysis revealed the interactions of exogenously introduced ROR1 with exogenous c-Src in COS-7 cells (Figure 5C) and endogenous c-Src in 293T cells (Figure S5B), whereas IP-WB analysis also revealed the interaction between endogenous ROR1 and c-Src proteins in NCI-H1975 cells (Figure 5D). In addition, an in vitro pull-down assay using GST-tagged ROR1 showed an interaction with endogenous c-Src in NCI-H1975 cell lysates (Figure S5C), as well as with a purified c-Src protein (Figure S5D). An in vitro ROR1 kinase assay using endogenous c-Src as a substrate in ROR1-negative NCI-H23 and 293T cells (Figures S5E and S5F), as well as exogenous kinase-dead c-Src the same as that in NIH/3T3 cells (Figure 5E), revealed robust c-Src phos-

phorylation. Furthermore, an association of ROR1 with the SH3 domain of c-Src was demonstrated by IP-WB analysis (Figure 5F), as well as by a GST pull-down assay (Figure S5G). In accordance with a previous report—in which it was reported that protein-protein interactions of c-Src are mediated by binding of its SH3 domain with proline-rich stretches of the binding partners (Yeatman, 2004)—the interaction between c-Src and ROR1 required the presence of the proline-rich domain but not kinase activity of ROR1 (Figure 5G). Whereas PTEN has been shown to be tyrosine-phosphorylated and negatively regulated by c-Src (Lu et al., 2003; Nagata et al., 2004), we observed a decrease tyrosine phosphorylation and S380/T382/T383 phosphorylation of PTEN in NCI-H1975 and SK-LC-5 cells with ROR1 knockdown (Figure S5H). ROR1 knockdown-induced growth inhibition was alleviated to a considerable extent by silencing of PTEN or p38 in NCI-H1975 cells (Figure 5H). Increase in c-Src phosphorylation in siPTEN-treated NCI-H1975 cells may reflect incomplete repression of PTEN activity, considering that PTEN dephosphorylates c-Src (Zhang et al., 2011). Although Wnt5a was recently suggested to mediate NF-κB signaling as an ROR1 ligand (Fukuda et al., 2008), our preliminary data suggest that this may not be the case in lung adenocarcinomas (Figures S5I and S5J).

## Dispensable c-Src Binding of ROR1 for ROR1-EGFR Association and Sustainment of EGFR-ERBB3 Interaction

We next examined whether c-Src binding of ROR1 is required to sustain ROR1-EGFR and EGFR-ERBB3 interactions. IP-WB analysis of COS-7 cells transiently cotransfected with various forms of ROR1 and EGFR revealed that the interaction between ROR1 and EGFR does not require either ROR1 kinase activity or the c-Src-interacting proline-rich domain of ROR1 (Figure 6A). Similarly, whereas an EGF-induced interaction between EGFR and ERBB3 was markedly enhanced by the presence of ROR1, both kinase activity and a proline-rich domain of ROR1 were shown to be dispensable for these interactions (Figure 6B). In addition, c-Src knockdown did not cause any appreciable changes in the interaction between ROR1 and EGFR or between EGFR and ERBB3 (Figure 6C). Thus, the present findings suggest that ROR1 mediates survival signals, at least in part, by two distinct mechanisms: ROR1 kinase-dependent c-Src-mediated signaling and ROR1-kinase independent sustainment of EGFR-ERBB3-PI3K signaling. In this regard, it is interesting that rescue from siROR1-mediated effects by introduction of exogenous wild-type ROR1 with silent mutations at the siRNA binding site was significantly counteracted by concurrent treatment with sic-Src in both NCI-H1975 and NCI-H358, whereas such rescue was significantly counteracted by concurrent treatment with siERBB3 in only NCI-H1975 but not NCI-H358 cells (Figure 7A), suggesting possible cellular context-dependent differences in contributions of ROR1-sustained downstream signaling. This finding also appeared to be consistent with differential sensitivity to sic-Src and siERBB3 treatment between NCI-H1975 and NCI-H358 cells (Figure S6A). The relative insensitivity to siERBB3 of NCI-H358 cells with a K-ras mutation may be consistent with a previous report of the ineffectiveness of treatment with a PI3K inhibitor alone in lung adenocarcinomas occurring in K-ras transgenic mice (Engelman et al., 2008). It was
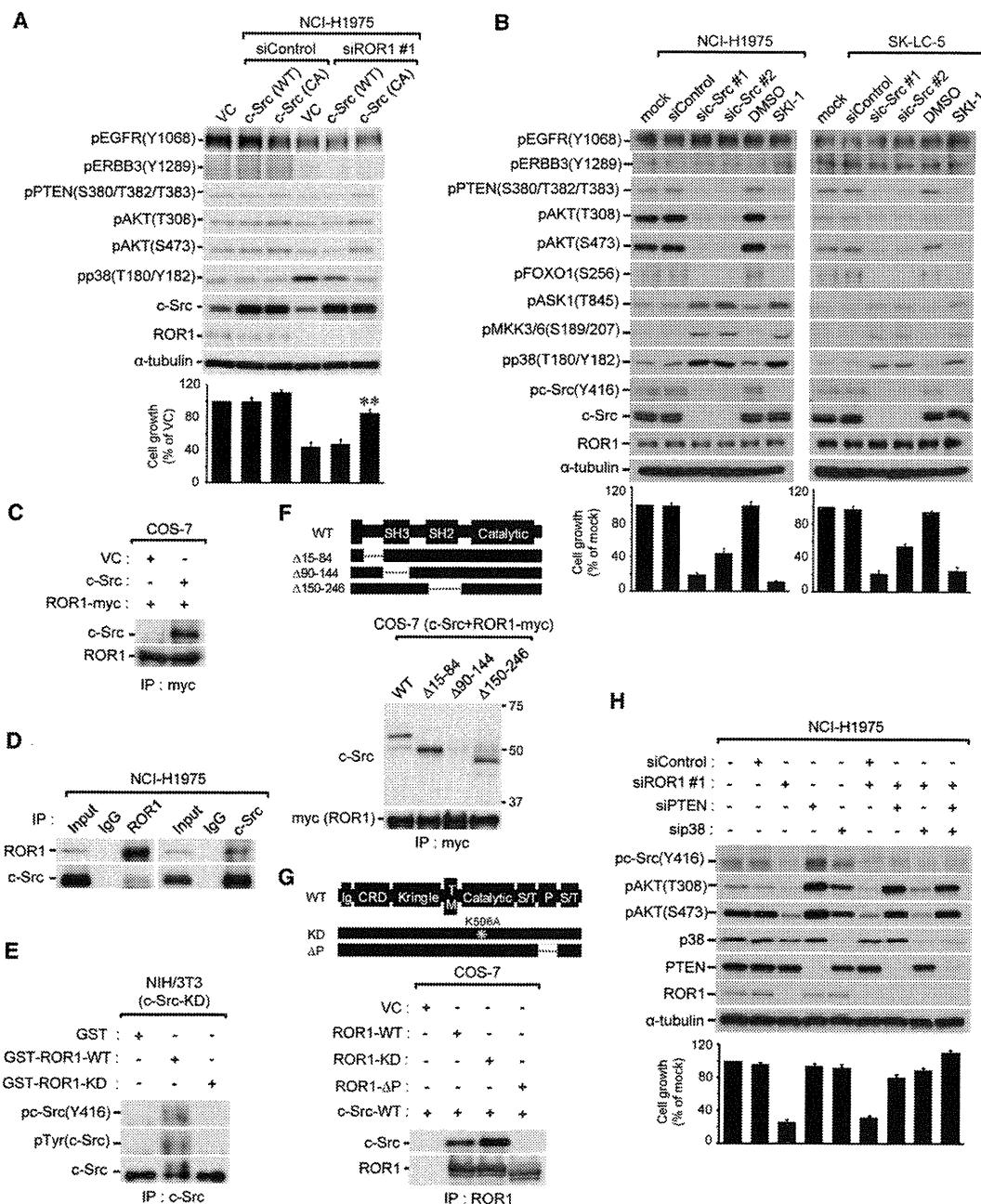
**Figure 5. ROR1 Binds to and Phosphorylates c-Src**

(A) WB (top panel) and colorimetric (bottom panel) analyses of NCI-H1975 cells introduced with siROR1 and c-Src. VC, empty vector control; WT, wild-type c-Src; CA, constitutive active c-Src. Data are shown as the mean ± SD (n = 3). **p < 0.001 versus VC+siROR1#1, as determined by Student's t test.

(B) Western blot (top panel) and colorimetric (bottom panel) analyses showing effects of c-Src inactivation by either siRNAs or a c-Src inhibitor (SKI-1). Data are shown as the mean ± SD (n = 3).

(C) IP-WB analysis of the interaction between exogenous ROR1 and c-Src in COS-7.

(D) IP-WB analysis of endogenous ROR1 and c-Src using cell lysates of NCI-H1975. IgG, negative control.

(E) In vitro ROR1 kinase assay using immunoprecipitated as a substrate in kinase-dead c-Src-transfected NIH/3T3.

(F) IP-WB analysis of the ROR1-c-Src interaction using COS-7 cotransfected with myc-tagged ROR1 and various deletion mutants of c-Src.

(G) IP-WB analyses of the ROR1-c-Src interaction using mutant ROR1 constructs. WT, wild-type; KD, kinase-dead; ΔP, ROR1 lacking proline-rich region.

(H) WB (top panel) and colorimetric (bottom panel) analyses of NCI-H1975 cosilenced for ROR1, PTEN, and/or p38. Data are shown as the mean ± SD (n = 3). See also Figure S5.
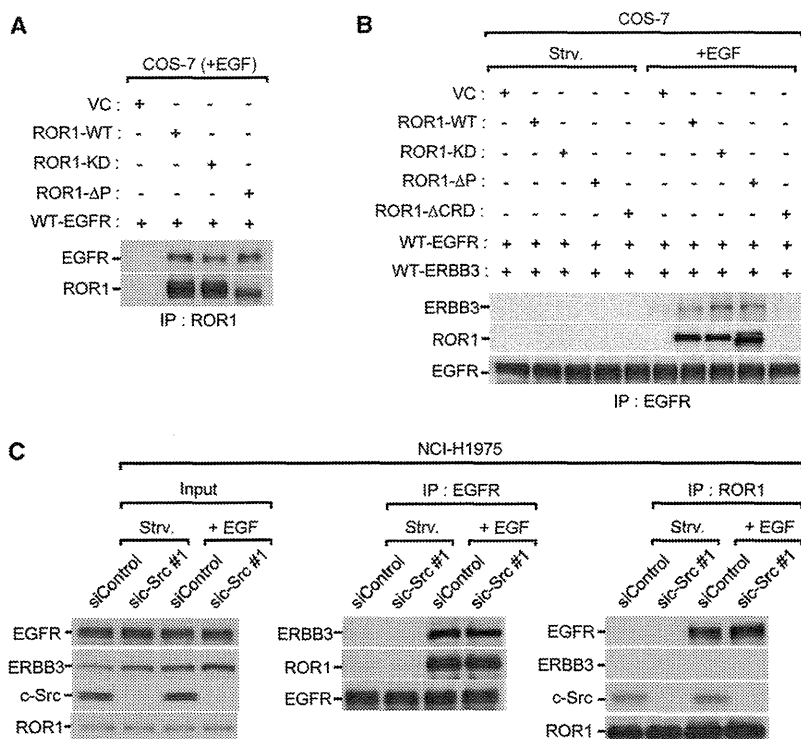
**A**



**B**



**C**



**Figure 6. ROR1 Sustains EGFR-ERBB3 Interaction Independent of c-Src Binding**

(A) IP-WB analysis of COS-7 cells co-introduced with EGFR and various forms of ROR1. WT, wild-type; KD, kinase-dead; ΔP, ROR1 lacking proline-rich region.

(B) IP-WB analysis of COS-7 cells co-introduced with various forms of ROR1, together with EGFR and ERBB3. Strv, serum starved.

(C) IP-WB analysis of the interactions among ROR1, EGFR, and ERBB3 in NCI-H1975 cells treated, with and without sic-Src. Strv, serum starved.

observed that sic-Src treatment in vivo similarly inhibited both growth and signaling in xenografts of two independent MSTO-211H clones overexpressing ROR1, supporting the notion that c-Src plays a crucial role as a downstream effector in this setting (Figures 7B and S6B).

## ROR1 Inhibition as a Therapeutic Option Irrespective of EGFR Status

It is of particular interest that ROR1 knockdown inhibited the growth of NCI-H1975 cells, because this line carries double EGFR mutations L858R and T790M, the latter of which is a well-recognized mutation that confers resistance to EGFR TKI (Kobayashi et al., 2005; Pao et al., 2005). We similarly observed growth inhibition by ROR1 knockdown in another EGFR TKI-resistant lung adenocarcinoma cell line, NCI-H820, which carries delE746-T751 and T790M EGFR mutations, together with MET amplification (Figures 8A and S7A; Bean et al., 2007; Engelman et al., 2007; Turke et al., 2010). HGF overexpression has been postulated as an additional mechanism for resistance to EGFR TKI by switching dependency from EGFR to MET (Yano et al., 2008). However, treatment with siROR1 overcame HGF-mediated resistance to gefitinib in the PC-9 lung adenocarcinoma cell line with an activating EGFR mutation, which was accompanied with reduction in HGF-elicited MET-transduced increase in AKT phosphorylation, as well as decreased c-Src and increased p38 phosphorylations (Figure 8B). It was also noted that siROR1 treatment enhanced growth inhibition in PC-9 cells when applied along with gefitinib in the absence of HGF (Figure S7B). Whereas gefitinib diminished ERBB3 phosphorylation to a nearly negligible level in the NCI-H358 lung adenocarcinoma cell line, which is known to be relatively sensitive to gefitinib despite wild-type

EGFR status (Engelman et al., 2005), concurrent siROR1 treatment with gefitinib further enhanced inhibition of cell growth in association with a clear reduction in remaining AKT phosphorylation (Figure 8C). Together, these findings suggest that ROR1 inhibition may be a therapeutic option for ROR1-positive lung adenocarcinomas irrespective of their EGFR status.

## DISCUSSION

Accumulated evidence indicates that NKX2-1, a lineage-specific transcription factor with essential roles in peripheral lung development (Maeda et al., 2007), is expressed in a major fraction of lung adenocarcinomas (Yatabe et al., 2002). Although previous studies, including ours, demonstrated the requirement of sustained NKX2-1 expression for lung adenocarcinoma survival (Kendall et al., 2007; Kwei et al., 2008; Tanaka et al., 2007; Weir et al., 2007), the mechanism by which NKX2-1 mediates, survival signals remains elusive. The present study clearly showed that ROR1 is a direct transcriptional target of NKX2-1 and is crucially involved in sustainment of a favorable balance between prosurvival PI3K-AKT signaling and the pro-apoptotic p38 pathway (Figures 8D), collapse of which elicits "oncogenic shock" (Sharma et al., 2006). Our previous studies revealed a significant association of NKX2-1 expression with EGFR mutations in lung adenocarcinomas (Takeuchi et al., 2006; Yatabe et al., 2005), suggesting their potential functional linkage. In this regard, the present findings suggest that NKX2-1 and EGFR may be functionally interrelated with each other through NKX2-1-mediated ROR1 induction in lung adenocarcinoma cells, which conceivably contributes to the development of lung adenocarcinomas with characteristic features. In addition, when considering the significant, yet incomplete, rescue from siNKX2-1-induced growth inhibition by ROR1 overexpression, an additional downstream target(s) may be involved in NKX2-1-mediated survival signaling.

The present results also demonstrate that ROR1 employs distinct kinase-dependent and -independent mechanisms to sustain a favorable balance between PI3K-AKT-mediated prosurvival signaling and the pro-apoptotic p38 pathway (Figure 8D). EGFR exists in a conformation that is unable to interact with ERBB3 and requires a ligand-engagement-elicited conformational change of the extracellular domain for dimerization-competence acquisition (Linggi and Carpenter, 2006). We found
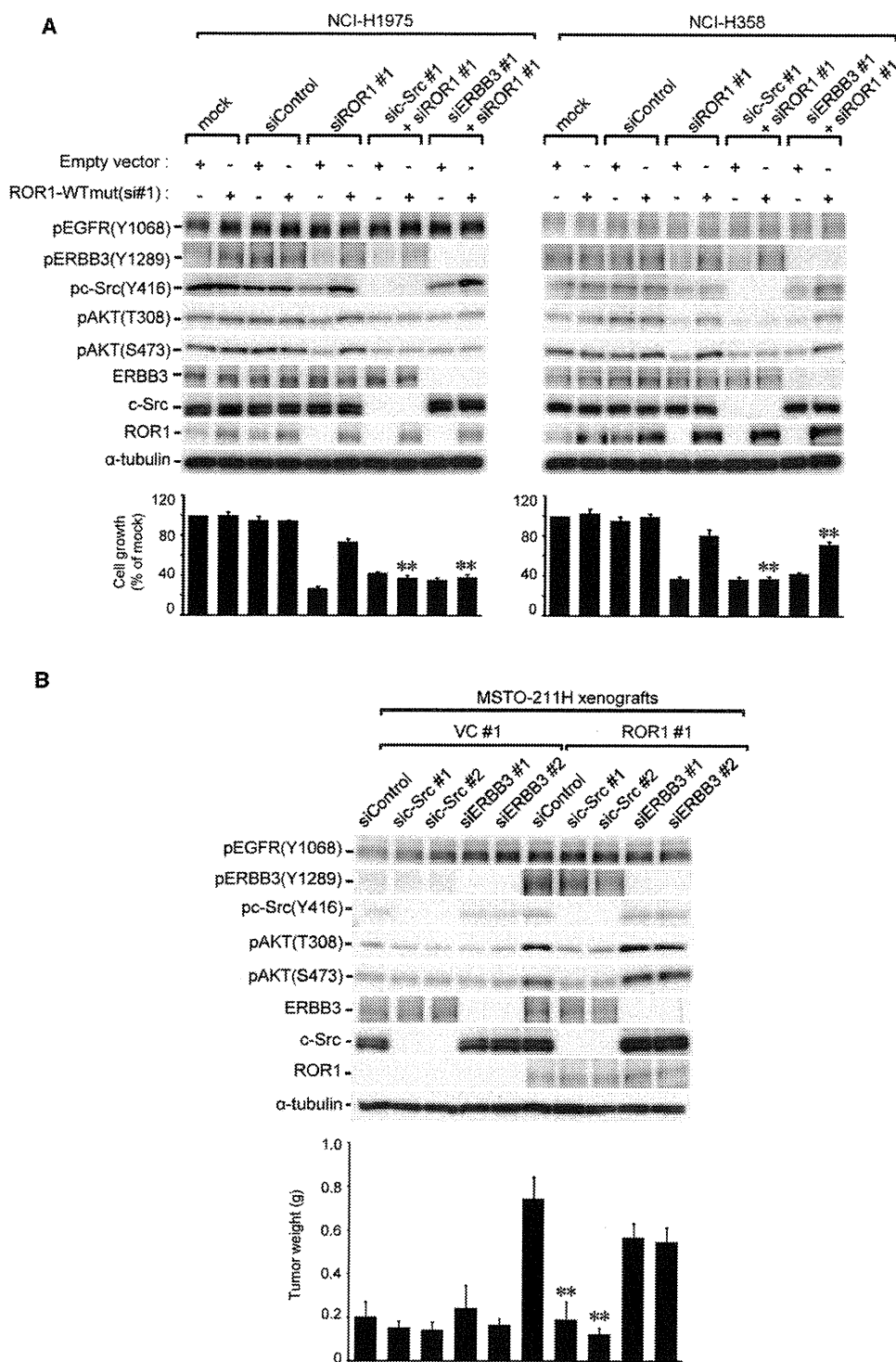
**Figure 7. ROR1 Sustains Downstream Signaling via c-Src and ERBB3 in a Cellular Context-Dependent Manner**

(A) Colorimetric assay (bottom panel) and WB analysis (top panel) of NCI-H1975 and NCI-H358 cells introduced with RNAi-resistant wild-type ROR1 [ROR1-mut(si#1)] and treated with siROR1, along with either sic-Src or siERBB3. Data are shown as the mean ± SD (n = 3). **p < 0.001 versus siROR1#1+ROR1-WTmut(si#1), as determined by Student's t test.

(B) In vivo tumor growth assay (bottom panel) and WB analysis (top panel) of xenografts of MSTO-211H, stably expressing exogenous ROR1, which were treated in vivo with sic-Src or siERBB3. Data are shown as the mean ± SD (n = 6). **p < 0.001 versus siControl +ROR1, as determined by Student's t test. See also Figure S6.
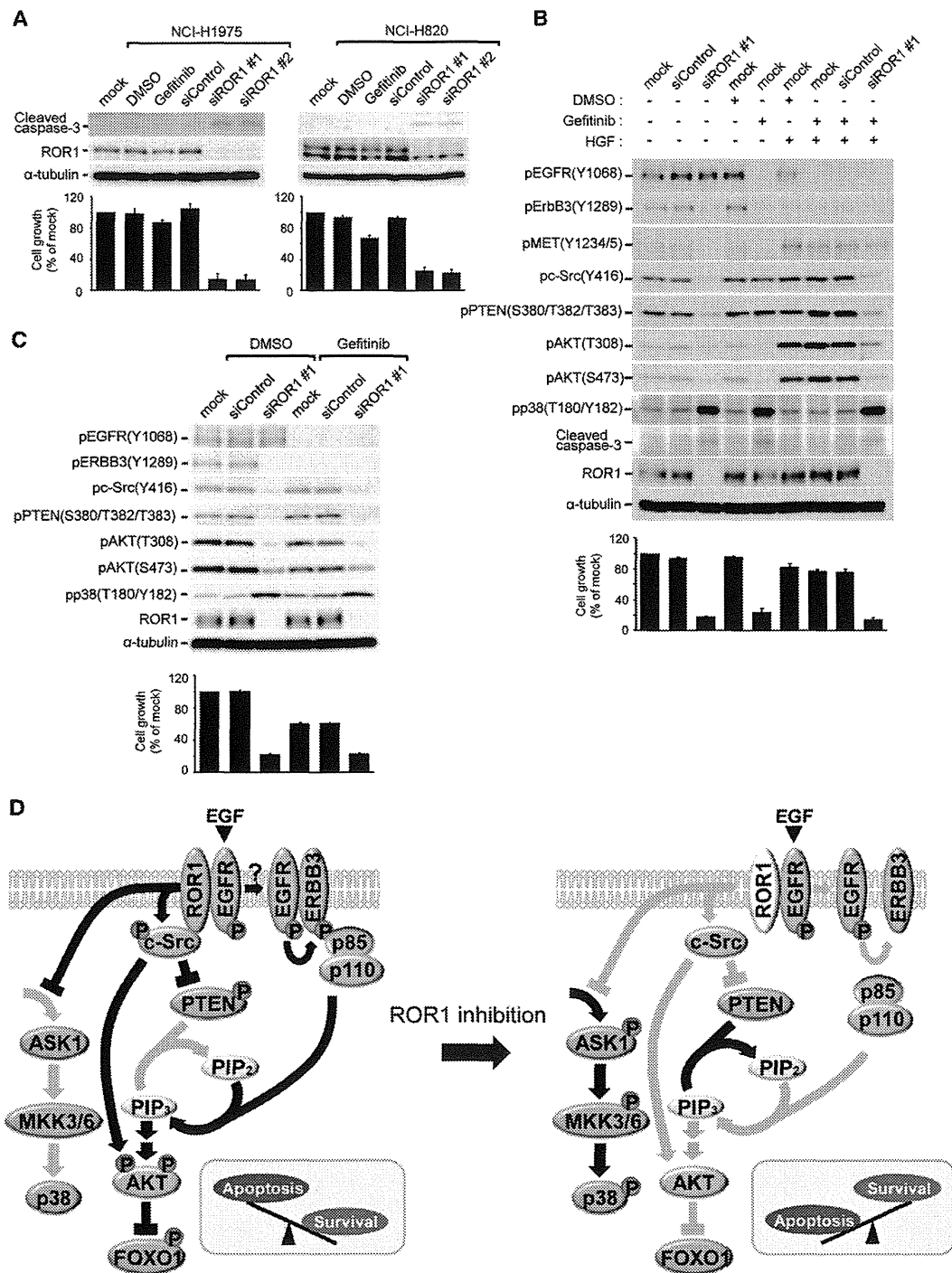
- 45 -

**Figure 8. ROR1 Repression Inhibits Lung Adenocarcinomas, Irrespective of the EGFR Status**

(A) WB analysis of cleaved caspase-3 (top panel) and a colorimetric assay (bottom panel) of NCI-H1975 and NCI-H820 knocked down for ROR1. Data are shown as the mean ± SD (n = 3).

(B) WB analysis of downstream molecules and a colorimetric assay of gefitinib and/or HGF treatment of siROR1-teated PC-9 cells. Data are shown as the mean ± SD (n = 3).

(C) Effects of siROR1 treatment in the relatively gefitinib-sensitive lung adenocarcinoma cell line NCI-H358. Data are shown as the mean ± SD (n = 3).

(D) Proposed model of how ROR1 plays a key role in sustaining a favorable balance between prosurvival and pro-apoptotic signaling. Two distinct mechanisms appear to coexist in sustaining prosurvival signaling: (1) ROR1 kinase-dependent c-Src activation and (2) kinase-independent sustainment of EGFR-ERBB3 association and consequential ERBB3 phosphorylation. See also Figure S7.

that ROR1 plays a role independent of its kinase activity in sustainment of EGF-induced signaling of the EGFR-ERBB3-PI3K axis, which is well known to play a crucial role in lung adenocarcinomas. Interestingly, we also observed that EGF treatment elicited robust phosphorylations of both EGFR at Y1068 and ERK, even in cells knocked down for ROR1. These findings indicate that ROR1 interaction with EGFR is selectively required for sustainment of signaling along the EGFR-ERBB3-PI3K axis through EGFR-ERBB3 heterodimerization and resultant ERBB3 phosphorylation but not for signaling toward the ERK pathway through autophosphorylation and homodimerization of EGFR. It is anticipated that future studies detailing the high-resolution structures of these receptors would provide insight into how ROR1 participates in this process with such specificity.

We previously showed that ROR1 physically interacts with and phosphorylates c-Src, which is a critical component of multiple signaling pathways important for cancer development (Yeatman, 2004). In addition, we noted that PTEN negative regulation of PI3K-AKT signaling appears to be, at least in part, under the influence of ROR1 expression, a finding consistent with previous reports on PTEN as a c-Src substrate (Lu et al., 2003; Nagata et al., 2004). It is also interesting to note that c-Src-mediated tyrosine phosphorylation has been proposed to trigger T308 and S473 phosphorylations by PDK1 and mTORC2, respectively, leading to AKT activation (Bellacosa et al., 1998; Chen et al., 2001; Jiang and Qiu, 2003) and lending support for the notion that ROR1-mediated c-Src activation may be also involved in this prerequisite process for robust AKT activation in lung adenocarcinoma cells. Thus, ROR1 appears to play a role independent of kinase activity in sustainment of EGF-induced signaling through the EGFR-ERBB3-PI3K axis, which is further upheld by ROR1 downstream through its kinase-dependent c-Src activation. It is also possible that there may be additional substrates of ROR1, as is generally the case in receptor tyrosine kinase signaling.

Taken together, the present findings identify ROR1 as an "Achilles' heel" in lung adenocarcinomas. Mechanisms, such as secondary EGFR mutation, MET amplification, and HGF overexpression, may arise in lung adenocarcinomas in patients undergoing EGFR-TKI treatment, leading to resistance to treatment by the tumors. The existence of such diverse mechanisms make it difficult to predict which should be targeted to prevent expansion of resistant clones (Bean et al., 2007; Engelman et al., 2007; Turke et al., 2010; Yano et al., 2008). From a clinical point of view, it is of particular interest that ROR1 inhibition appears to be effective for treatment of gefitinib-resistant lung adenocarcinomas with various resistance mechanisms. To date, very little is known about the functions of ROR1 and its role in human cancers, in accordance with its name, that is, tyrosine kinase-like orphan receptor 1 (Forrester, 2002; Green et al., 2008; Minami et al., 2010). Interestingly, upregulation of ROR1 was recently reported in chronic lymphocytic leukemia (Baskar et al., 2008; Daneshmanesh et al., 2008; Fukuda et al., 2008). In addition, it is notable that NKX2-1 is expressed in small cell lung cancers at a high frequency (Kitamura et al., 2009). Future development of therapeutic means including ROR1-specific antibodies and small molecules that inhibit both or either of the two distinct prosurvival signal-sustaining functions is greatly anticipated for attempts to reduce the intolerable

death toll from currently "hard-to-cure" lung adenocarcinomas, as well as possibly other ROR1-positive cancers.

## EXPERIMENTAL PROCEDURES

### Cell Lines and Tissues

NCI-H1975, NCI-H820, NCI-H441, NCI-H358, NCI-H23, and PC-9 cells were purchased from the American Type Culture Collection. The derivations and culture conditions of other human cancer cell lines, as well as the immortalized human lung epithelial cell line HPL1D, have been reported (Tanaka et al., 2007). Their characteristics are summarized in Table S1. Human cancer and normal tissues as well as primary normal lung epithelial cells were obtained under approval from the institutional review board of Nagoya University with written informed consent from each patient.

### Constructs

The methods used for the construction of the expression constructs of full-length human NKX2-1 cDNA in pCMV-puro (pCMVpuro-NKX2-1), as well as of short hairpin RNA (shRNA) against NKX2-1 in pH1RNAneo (pH1RNAneo-shNKX2-1), have been described (Tanaka et al., 2007). Full-length human ROR1 cDNA (OriGene Technologies, Rockville, MDs) was inserted into a pCMV-puro vector, and the entire open reading frame of the resulting construct (pCMVpuro-ROR1) was thoroughly sequenced. pCMVpuro-ROR1-KD (an inactivating K506A mutation at the ATP binding site), pCMVpuro-ROR1-ΔP, and pCMVpuro-ROR1-ΔCRD were constructed by in vitro mutagenesis using KOD-plus-DNA polymerase (Toyobo, Osaka, Japan). In addition, a myc-tagged derivative of pIRESpuro2-ROR1 (pIRESpuro2-ROR1-myc) and its derivatives (pIRESpuro2-ROR1-ΔN-myc and pIRESpuro2-ROR1-ΔC-myc) were constructed. pIRESpuro2-ROR1-Δlg-myc, pIRESpuro2-ROR1-ΔCRD-myc, pIRESpuro2-ROR1-ΔKringle-myc, pIRESpuro2-ROR1-Δlg+CRD-myc, pIRESpuro2-ROR1-ΔCRD+Kringle-myc, and pIRESpuro2-ROR1-Δlg+CRD+Kringle-myc were also constructed by in vitro mutagenesis using a KOD-plus-DNA polymerase.

Full-length human EGFR cDNA was purchased from Riken and inserted into a pCMV-puro vector (pCMVpuro-EGFR). Full-length human ERBB3 cDNA (pcDNA5/FRT-ERBB3) was kindly provided by N. Taniguchi (Osaka University, Osaka, Japan). pNeo-MSV-c-Src wild-type (WT), constitutive active (CA), and kinase dead (KD) were kindly provided by T. Hunter (Salk Institute, La Jolla, CA; Broome and Hunter, 1996), and the inserts were transferred into pCMVpuro, resulting in the following: pCMVpuro-WT-c-Src, pCMVpuro-CA-c-Src, and pCMVpuro-KD-c-Src. pRC-CMV-c-Src wild-type (WT), Δ15-84 (Δ15), Δ90-144 (Δ90), and Δ150-246 (Δ150) were kindly provided by S.J. Shattil (University of California San Diego, San Diego, CA, USA; Arias-Salgado et al., 2003).

### Microarray Analysis

HPL1D cells stably expressing NKX2-1 (HPL1D-NKX2-1) were generated by transfecting pCMVpuro-NKX2-1 using FuGENE6, followed by puromycin selection. RNA was extracted from HPL1D-NKX2-1 and its empty control vector HPL1D-VC and then analyzed in dye-swapped duplicate using a low RNA fluorescent linear amplification kit and 44K whole human genome microarrays (Agilent Technologies, Santa Clara, CA), in accordance with the manufacturer's instructions. HPL1D cells were also transiently transfected with NKX2-1, selected with puromycin for three days, and harvested for validation of ROR1 induction by western blot analysis.

### Western Blot and Immunoprecipitation-Western Blot Analyses

Western blot and immunoprecipitation-western blot analyses were performed using standard procedures with Immobilon-P filters (Millipore, Billerica, MA) and an enhanced chemiluminescence system (GE Healthcare, Buckinghamshire, UK). For analysis of physical interactions between ROR1 and c-Src, pIRESpuro2-ROR1-myc was transfected with various c-Src expression constructs, including wild-type (WT), Δ15-84 (Δ15), Δ90-144 c-Src (Δ90), or Δ150-246 c-Src (Δ150). Similarly, wild-type c-Src was transfected with pCMVpuro-ROR1 (ROR1), pCMVpuro-ROR1-K506A (ROR1-KD), or pCMVpuro-ROR1-ΔP (ROR1-ΔP). Cells were harvested 24 hr after transfection with the lysis buffer containing 20 mM Tris-HCl (pH 7.5), 150 mM NaCl,

1 mM EDTA, 1 mM EGTA, 1% Triton X-100, 2.5 mM sodium pyrophosphate, 1 mM β-glycerophosphate, 1 mM $Na_3VO_4$, 1 μg/ml leupeptin, 1 mM PMSF, and Complete (EDTA-free protease inhibitor mixture; Roche, Mannheim, Germany). For analysis of physical interactions among ROR1, EGFR, and ERBB3, pCMVpuro-EGFR and/or pcDNA5/FRT-ERBB3 were transfected with various ROR1 expression constructs, including wild-type (WT), ΔN, ΔC, ΔIg, ΔCRD, ΔKringle, ΔIg+CRD, ΔCRD+Kringle, and ΔIg+CRD+Kringle. Cells were serum-starved for 24 hr, treated with 20 ng/ml of EGF 48 hr after transfection for up to 30 min, and then harvested to analyze their interactions through immunoprecipitation-western blot analysis. A NP-40 lysis buffer containing 20 mM Tris-HCl (pH 8.0), 137 mM NaCl, 2 mM EDTA, 1% NP-40, 10% Glycerol, and 1 mM $Na_3VO_4$ was used to investigate the physical interactions among ROR1, EGFR, and ERBB3.

## Clarification of ROR1-RNAi Effects

pCMVpuro-ROR1-WT-mut(si#1) and pCMVpuro-ROR1-KD-mut(si#1), which carry multiple silent mutations at the binding site of siROR1#1, were constructed by in vitro mutagenesis using KOD-plus-DNA Polymerase (Toyobo) and the oligonucleotide primer 5'-CAACAGTGGACAGAGTTCCAG-3' (mutated residues are underlined). NCI-H1975 and NCI-H358 at $2.0 \times 10^6$ were transfected with an empty pCMVpuro vector (VC), pCMVpuro-ROR1 (ROR1), pCMVpuro-ROR1-WT-mut(si#1) [ROR1-WT-mut(si#1)], or pCMVpuro-ROR1-KD-mut(si#1) [ROR1-KD-mut(si#1)], followed by puromycin selection (1.5 μg/ml) for three days. The resulting bulk transfectants were then re-seeded into 6-well plates and further introduced with siROR1 alone or along with either sic-Src or siERBB3 on the next day. Cells were harvested for western blot analysis at three days or a colorimetric assay at five days after siRNA transfection. For rescue experiments of ERBB3 phosphorylation, NCI-H1975 cells expressing ROR1-WT-mut(si#1) or ROR1-KD-mut(si#1) were transfected with siROR1 or siControl and then serum-starved for 24 hr. After treatment with 20 ng/ml of EGF for various time periods, western blot analyses were performed.

## Analyses of Functional Relationships of ROR1 with NKX2-1 and c-Src

In order to analyze the effects of exogenous ROR1 expression in shNKX2-1-treated lung adenocarcinoma cells, pH1RNAneo-shNKX2-1 and pCMVpuro-ROR1 were cotransfected into NCI-H358 at a ratio of 1:4, followed by neomycin selection for two weeks before counting the number of colonies. The functional relationship between ROR1 and c-Src was analyzed in NCI-H1975 cells by transfection of pCMVpuro-WT-c-Src or pCMVpuro-CA-c-Src; then, transfected cells were selected with puromycin for three days. The resulting bulk transfectants were then re-seed into 6-well plates and further introduced with siROR1 or siControl. Cells were harvested for western blot analysis at 72 hr after siRNA transfection. A colorimetric assay was performed five days after siRNA transfection. NCI-H1975, SK-LC-5, and NCI-H23 cells were also treated with the Src kinase inhibitor SKI-1 at 5 μM for 6 hr and harvested for western blot analysis. For a colorimetric assay, cells were treated with 5 μM SKI-1 for five days.

## In Vivo Tumorigenicity Assays

NCI-H1975 cells at $1.0 \times 10^7$ were subcutaneously inoculated into the lower flanks of 8-week-old athymic nude mice (Japan SLC, Shizuoka, Japan). One week after inoculation, a mixture of 1 nmol of siRNAs (siROR1 #1, #2, and #3) and 200 μl of atelocollagen (Koken, Tokyo, Japan) was injected into the tumors, which had an average volume of 50 mm³. Tumor weights were measured two weeks after siRNA injection. In vivo tumorigenicity assays were also performed by subcutaneous inoculation of $1.0 \times 10^7$ MSTO-211H cells stably expressing wild-type ROR1 (ROR1#1 and #2), kinase-dead ROR1 (ROR1-KD#1 and #2), or those introduced with an empty vector (VC#1 and #2) into the lower flanks of 8-week-old athymic nude mice (Japan SLC). In this experiment, tumor weights were determined three weeks after inoculation. In addition, tumors were analyzed by western blot analysis for detection of various protein expressions. For analysis of the effects of c-Src or ERBB3 knockdown in the ROR1 transfectants, a mixture of 1 nmol siRNAs (siControl, sic-Src #1, sic-Src #2, siERBB3 #1, or siERBB3 #2) and 200 μl atelocollagen was injected into the tumors at one week after inoculation. Tumor weights

were measured two weeks after siRNA injection and various protein expressions were analyzed by western blot analysis. All animal experiments were performed in compliance with the regulations for animal experiments of Nagoya University.

## EGF, HGF, and/or Gefitinib Treatment in Cells Knocked Down for ROR1

NCI-H1975 and SK-LC-5 cells ($1.0 \times 10^5$) were transfected with 20 nM siROR1 or siControl and then serum-starved for 24 hr. After treatment with 20 ng/ml of EGF for various time periods, western blot and immunofluorescent staining analyses were performed. NCI-H1975, NCI-H820, and NCI-H358 cells ($1.0 \times 10^5$) were transfected with 20 nM siROR1 or siControl, then cultured for three days before treatment with 1 μM gefitinib for 6 hr, and harvested for western blot analysis. For a colorimetric assay, cells ($5.0 \times 10^4$) were transfected with the siRNAs and then continuously exposed to 1 μM gefitinib for four days. Similarly, three days after siRNA transfection, PC-9 cells were treated with 1 μM gefitinib and/or 50 ng/ml of HGF for 6 hr and then harvested for western blot analysis. Effects on cell proliferation were also examined by a colorimetric assay after a four-day exposure to 1 μM gefitinib and/or 50 ng/ml of HGF, which was initiated the day after siRNA transfection.

## ACCESSION NUMBERS

The raw microarray data have been deposited in the Gene Expression Omnibus databases under accession number GSE25830.

## SUPPLEMENTAL INFORMATION

Supplemental Information includes seven figures, one table, and Supplemental Experimental Procedures and can be found with this article online at doi:10.1016/j.ccr.2012.02.008.

## REFERENCES

Arias-Salgado, E.G., Lizano, S., Sarkar, S., Brugge, J.S., Ginsberg, M.H., and Shattil, S.J. (2003). Src kinase activation by direct interaction with the integrin beta cytoplasmic domain. Proc. Natl. Acad. Sci. USA 100, 13298–13302.

Baskar, S., Kwong, K.Y., Hofer, T., Levy, J.M., Kennedy, M.G., Lee, E., Staudt, L.M., Wilson, W.H., Wiestner, A., and Rader, C. (2008). Unique cell surface expression of receptor tyrosine kinase ROR1 in human B-cell chronic lymphocytic leukemia. Clin. Cancer Res. 14, 396–404.

Bean, J., Brennan, C., Shih, J.Y., Riely, G., Viale, A., Wang, L., Chitale, D., Motoi, N., Szoke, J., Broderick, S., et al. (2007). MET amplification occurs with or without T790M mutations in EGFR mutant lung tumors with acquired resistance to gefitinib or erlotinib. Proc. Natl. Acad. Sci. USA 104, 20932–20937.

Bellacosa, A., Chan, T.O., Ahmed, N.N., Datta, K., Malstrom, S., Stokoe, D., McCormick, F., Feng, J., and Tsichlis, P. (1998). Akt activation by growth factors is a multiple-step process: the role of the PH domain. Oncogene 17, 313–325.

- 48 -

Boggaram, V. (2009). Thyroid transcription factor-1 (TTF-1/Nkx2.1/TITF1) gene regulation in the lung. Clin. Sci. *116*, 27–35.

Broome, M.A., and Hunter, T. (1996). Requirement for c-Src catalytic activity and the SH3 domain in platelet-derived growth factor BB and epidermal growth factor mitogenic signaling. J. Biol. Chem. *271*, 16798–16806.

Calnan, D.R., and Brunet, A. (2008). The FoxO code. Oncogene *27*, 2276–2288.

Chen, R., Kim, O., Yang, J., Sato, K., Eisenmann, K.M., McCarthy, J., Chen, H., and Qiu, Y. (2001). Regulation of Akt/PKB activation by tyrosine phosphorylation. J. Biol. Chem. *276*, 31858–31862.

Daneshmanesh, A.H., Mikaelsson, E., Jeddi-Tehrani, M., Bayat, A.A., Ghods, R., Ostadkarampour, M., Akhondi, M., Lagercrantz, S., Larsson, C., Osterborg, A., et al. (2008). Ror1, a cell surface receptor tyrosine kinase is expressed in chronic lymphocytic leukemia and may serve as a putative target for therapy. Int. J. Cancer *123*, 1190–1195.

Engelman, J.A., Jänne, P.A., Mermel, C., Pearlberg, J., Mukohara, T., Fleet, C., Cichowski, K., Johnson, B.E., and Cantley, L.C. (2005). ErbB-3 mediates phosphoinositide 3-kinase activity in gefitinib-sensitive non-small cell lung cancer cell lines. Proc. Natl. Acad. Sci. USA *102*, 3788–3793.

Engelman, J.A., Zejnullahu, K., Mitsudomi, T., Song, Y., Hyland, C., Park, J.O., Lindeman, N., Gale, C.M., Zhao, X., Christensen, J., et al. (2007). MET amplification leads to gefitinib resistance in lung cancer by activating ERBB3 signaling. Science *316*, 1039–1043.

Engelman, J.A., Chen, L., Tan, X., Crosby, K., Guimaraes, A.R., Upadhyay, R., Maira, M., McNamara, K., Perera, S.A., Song, Y., et al. (2008). Effective use of PI3K and MEK inhibitors to treat mutant Kras G12D and PIK3CA H1047R murine lung cancers. Nat. Med. *14*, 1351–1356.

Forrester, W.C. (2002). The Ror receptor tyrosine kinase family. Cell. Mol. Life Sci. *59*, 83–96.

Fukuda, T., Chen, L., Endo, T., Tang, L., Lu, D., Castro, J.E., Widhopf, G.F., 2nd, Rassenti, L.Z., Cantwell, M.J., Prussak, C.E., et al. (2008). Antisera induced by infusions of autologous Ad-CD154-leukemia B cells identify ROR1 as an oncofetal antigen and receptor for Wnt5a. Proc. Natl. Acad. Sci. USA *105*, 3047–3052.

Garraway, L.A., and Sellers, W.R. (2006). Lineage dependency and lineage-survival oncogenes in human cancer. Nat. Rev. Cancer *6*, 593–602.

Green, J.L., Kuntz, S.G., and Sternberg, P.W. (2008). Ror receptor tyrosine kinases: orphans no more. Trends Cell Biol. *18*, 536–544.

Hennessy, B.T., Smith, D.L., Ram, P.T., Lu, Y., and Mills, G.B. (2005). Exploiting the PI3K/AKT pathway for cancer drug discovery. Nat. Rev. Drug Discov. *4*, 988–1004.

Jiang, T., and Qiu, Y. (2003). Interaction between Src and a C-terminal proline-rich motif of Akt is required for Akt activation. J. Biol. Chem. *278*, 15789–15793.

Kendall, J., Liu, Q., Bakleh, A., Krasnitz, A., Nguyen, K.C., Lakshmi, B., Gerald, W.L., Powers, S., and Mu, D. (2007). Oncogenic cooperation and coamplification of developmental transcription factor genes in lung cancer. Proc. Natl. Acad. Sci. USA *104*, 16663–16668.

Kimura, S., Hara, Y., Pineau, T., Fernandez-Salguero, P., Fox, C.H., Ward, J.M., and Gonzalez, F.J. (1996). The T/ebp null mouse: thyroid-specific enhancer-binding protein is essential for the organogenesis of the thyroid, lung, ventral forebrain, and pituitary. Genes Dev. *10*, 60–69.

Kitamura, H., Yazawa, T., Sato, H., Okudela, K., and Shimoyamada, H. (2009). Small cell lung cancer: significance of RB alterations and TTF-1 expression in its carcinogenesis, phenotype, and biology. Endocr. Pathol. *20*, 101–107.

Kobayashi, S., Boggon, T.J., Dayaram, T., Jänne, P.A., Kocher, O., Meyerson, M., Johnson, B.E., Eck, M.J., Tenen, D.G., and Halmos, B. (2005). EGFR mutation and resistance of non-small-cell lung cancer to gefitinib. N. Engl. J. Med. *352*, 786–792.

Kwei, K.A., Kim, Y.H., Girard, L., Kao, J., Pacyna-Gengelbach, M., Salari, K., Lee, J., Choi, Y.L., Sato, M., Wang, P., et al. (2008). Genomic profiling identifies TITF1 as a lineage-specific oncogene amplified in lung cancer. Oncogene *27*, 3635–3640.

Linggi, B., and Carpenter, G. (2006). ErbB receptors: new insights on mechanisms and biology. Trends Cell Biol. *16*, 649–656.

Lu, Y., Yu, Q., Liu, J.H., Zhang, J., Wang, H., Koul, D., McMurray, J.S., Fang, X., Yung, W.K., Siminovitch, K.A., and Mills, G.B. (2003). Src family protein-tyrosine kinases alter the function of PTEN to regulate phosphatidylinositol 3-kinase/AKT cascades. J. Biol. Chem. *278*, 40057–40066.

Maeda, Y., Davé, V., and Whitsett, J.A. (2007). Transcriptional control of lung morphogenesis. Physiol. Rev. *87*, 219–244.

Martin, G.S. (2001). The hunting of the Src. Nat. Rev. Mol. Cell Biol. *2*, 467–475.

Masuda, A., Kondo, M., Saito, T., Yatabe, Y., Kobayashi, T., Okamoto, M., Suyama, M., Takahashi, T., and Takahashi, T. (1997). Establishment of human peripheral lung epithelial cell lines (HPL1) retaining differentiated characteristics and responsiveness to epidermal growth factor, hepatocyte growth factor, and transforming growth factor beta1. Cancer Res. *57*, 4898–4904.

Minami, Y., Oishi, I., Endo, M., and Nishita, M. (2010). Ror-family receptor tyrosine kinases in noncanonical Wnt signaling: their implications in developmental morphogenesis and human diseases. Dev. Dyn. *239*, 1–15.

Nagata, Y., Lan, K.H., Zhou, X., Tan, M., Esteva, F.J., Sahin, A.A., Klos, K.S., Li, P., Monia, B.P., Nguyen, N.T., et al. (2004). PTEN activation contributes to tumor inhibition by trastuzumab, and loss of PTEN predicts trastuzumab resistance in patients. Cancer Cell *6*, 117–127.

Nishikawa, E., Osada, H., Okazaki, Y., Arima, C., Tomida, S., Tatematsu, Y., Taguchi, A., Shimada, Y., Yanagisawa, K., Yatabe, Y., et al. (2011). miR-375 is activated by ASH1 and inhibits YAP1 in a lineage-dependent manner in lung cancer. Cancer Res. *71*, 6165–6173.

Osada, H., Tatematsu, Y., Yatabe, Y., Horio, Y., and Takahashi, T. (2005). ASH1 gene is a specific therapeutic target for lung cancers with neuroendocrine features. Cancer Res. *65*, 10680–10685.

Osada, H., Tomida, S., Yatabe, Y., Tatematsu, Y., Takeuchi, T., Murakami, H., Kondo, Y., Sekido, Y., and Takahashi, T. (2008). Roles of achaete-scute homologue 1 in DKK1 and E-cadherin repression and neuroendocrine differentiation in lung cancer. Cancer Res. *68*, 1647–1655.

Pao, W., Miller, V.A., Politi, K.A., Riely, G.J., Somwar, R., Zakowski, M.F., Kris, M.G., and Varmus, H. (2005). Acquired resistance of lung adenocarcinomas to gefitinib or erlotinib is associated with a second mutation in the EGFR kinase domain. PLoS Med. *2*, e73.

Rothenberg, S.M., Engelman, J.A., Le, S., Riese, D.J., 2nd, Haber, D.A., and Settleman, J. (2008). Modeling oncogene addiction using RNA interference. Proc. Natl. Acad. Sci. USA *105*, 12480–12484.

Sharma, S.V., Gajowniczek, P., Way, I.P., Lee, D.Y., Jiang, J., Yuza, Y., Classon, M., Haber, D.A., and Settleman, J. (2006). A common signaling cascade may underlie "addiction" to the Src, BCR-ABL, and EGF receptor oncogenes. Cancer Cell *10*, 425–435.

Sharma, S.V., and Settleman, J. (2009). ErbBs in lung cancer. Exp. Cell Res. *315*, 557–571.

Takeuchi, T., Tomida, S., Yatabe, Y., Kosaka, T., Osada, H., Yanagisawa, K., Mitsudomi, T., and Takahashi, T. (2006). Expression profile-defined classification of lung adenocarcinoma shows close relationship with underlying major genetic changes and clinicopathologic behaviors. J. Clin. Oncol. *24*, 1679–1688.

Tanaka, H., Yanagisawa, K., Shinjo, K., Taguchi, A., Maeno, K., Tomida, S., Shimada, Y., Osada, H., Kosaka, T., Matsubara, H., et al. (2007). Lineage-specific dependency of lung adenocarcinomas on the lung development regulator TTF-1. Cancer Res. *67*, 6007–6011.

Turke, A.B., Zejnullahu, K., Wu, Y.L., Song, Y., Dias-Santagata, D., Lifshits, E., Toschi, L., Rogers, A., Mok, T., Sequist, L., et al. (2010). Preexistence and clonal selection of MET amplification in EGFR mutant NSCLC. Cancer Cell *17*, 77–88.

Weinstein, I.B. (2002). Cancer. Addiction to oncogenes—the Achilles heal of cancer. Science *297*, 63–64.

- 49 -

Weir, B.A., Woo, M.S., Getz, G., Perner, S., Ding, L., Beroukhim, R., Lin, W.M., Province, M.A., Kraja, A., Johnson, L.A., et al. (2007). Characterizing the cancer genome in lung adenocarcinoma. Nature *450*, 893–898.

Yano, S., Wang, W., Li, Q., Matsumoto, K., Sakurama, H., Nakamura, T., Ogino, H., Kakiuchi, S., Hanibuchi, M., Nishioka, Y., et al. (2008). Hepatocyte growth factor induces gefitinib resistance of lung adenocarcinoma with epidermal growth factor receptor-activating mutations. Cancer Res. *68*, 9479–9487.

Yatabe, Y., Mitsudomi, T., and Takahashi, T. (2002). TTF-1 expression in pulmonary adenocarcinomas. Am. J. Surg. Pathol. *26*, 767–773.

Yatabe, Y., Kosaka, T., Takahashi, T., and Mitsudomi, T. (2005). EGFR mutation is specific for terminal respiratory unit type adenocarcinoma. Am. J. Surg. Pathol. *29*, 633–639.

Yeatman, T.J. (2004). A renaissance for SRC. Nat. Rev. Cancer *4*, 470–480.

Zhang, S., Huang, W.C., Li, P., Guo, H., Poh, S.B., Brady, S.W., Xiong, Y., Tseng, L.M., Li, S.H., Ding, Z., et al. (2011). Combating trastuzumab resistance by targeting SRC, a common node downstream of multiple resistance pathways. Nat. Med. *17*, 461–469.

- 50 -

# MYBPH inhibits NM IIA assembly via direct interaction with NMHC IIA and reduces cell motility

Yasuyuki Hosono [a], Jiro Usukura [b], Tomoya Yamaguchi [a], Kiyoshi Yanagisawa [a], Motoshi Suzuki [a], Takashi Takahashi [a,*]

[a] Division of Molecular Carcinogenesis, Center for Neurological Diseases and Cancer, Nagoya University Graduate School of Medicine, Showa-ku, Nagoya 466-8550, Japan
[b] Division of Integrated Project, EcoTopia Science Institute, Nagoya University, Chikusa-ku, Nagoya 464-8603, Japan

## ARTICLE INFO

## ABSTRACT

Actomyosin filament assembly is a critical step in tumor cell migration. We previously found that myosin binding protein H (MYBPH) is directly transactivated by the TTF-1 lineage-survival oncogene in lung adenocarcinomas and inhibits phosphorylation of the myosin regulatory light chain (RLC) of non-muscle myosin IIA (NM IIA) via direct interaction with Rho kinase 1 (ROCK1). Here, we report that MYBPH also directly interacts with an additional molecule, non-muscle myosin heavy chain IIA (NMHC IIA), which was found to occur between MYBPH and the rod portion of NMHC IIA. MYBPH inhibited NMHC IIA assembly and reduced cell motility. Conversely, siMYBPH-induced increased motility was partially, yet significantly, suppressed by blebbistatin, a non-muscle myosin II inhibitor, while more profound effects were attained by combined treatment with siROCK1 and blebbistatin. Electron microscopy observations showed well-ordered paracrystals of NMHC IIA reflecting an assembled state, which were significantly less frequently observed in the presence of MYBPH. Furthermore, an in vitro sedimentation assay showed that a greater amount of NMHC IIA was in an unassembled state in the presence of MYBPH. Interestingly, treatment with a ROCK inhibitor that impairs transition of NM IIA from an assembly-incompetent to assembly-competent state reduced the interaction between MYBPH and NMHC IIA, suggesting that MYBPH has higher affinity to assembly-competent NM IIA. These results suggest that MYBPH inhibits RLC and NMHC IIA, independent components of NM IIA, and negatively regulates actomyosin organization at 2 distinct steps, resulting in firm inhibition of NM IIA assembly.

© 2012 Elsevier Inc. All rights reserved.

## 1. Introduction

Cell migration is a critical step in tumor invasion and metastasis, while the contractile motion of cancer cells is associated with continuous structural transitions between assembled and disassembled states of actomyosin bundles [1–3]. Non-muscle myosin II (NM II), a major component of the actomyosin cytoskeleton, is comprised of 2 non-muscle myosin heavy chain (NMHCs), 2 myosin essential light chains (ELCs), and 2 myosin regulatory light chains (RLCs). In human cells, 3 NMHCs (IIA, IIB, and IIC) are encoded by distinct genes (MYH9, MYH10, and MYH14, respectively) and constitute the NM II isoforms, which are named NM IIA, NM IIB, and NM IIC, respectively [4,5]. Accumulating evidence indicates that NM II members, especially NM IIA, play crucial roles in cancer cell migration via bivalent binding to and linking of actin filaments [6–8].

One of the major activators of the NM II assembly is Rho kinase 1 (ROCK1), a downstream effector of RhoA, which phosphorylates

RLC and induces subsequent unfolding of NM II into an assembly-competent form. This assembly-competent NM II is capable of NM II dimer formation via assembly of NMHC [9,10]. It has also been shown that RLC phosphorylation is crucially involved in cell morphogenesis and motility, as well as cancer invasion and metastasis [11–14]. In contrast, little is known about the regulatory mechanisms of the subsequent NMHC IIA assembly steps, while previous reports have focused on regulatory phosphorylation of NMHC by protein kinase C (PKC), casein kinase II (CK II), and transient receptor potential melastatin 7 (TRPM7) at the C-terminus of the NMHC [15,16].

TTF-1 is a lineage-specific transcription factor required for the development and the physiological functions of peripheral lung [17–19]. TTF-1 is also expressed in a major fraction of lung adenocarcinomas, which appears to reflect their derivation from the terminal respiratory unit [18,19]. We and others previously identified that TTF-1 also plays a role as a lineage-survival oncogene and exhibits focal amplification in lung adenocarcinomas [20–23]. In addition, we recently found that TTF-1 induces expression of the receptor tyrosine kinase-like orphan receptor 1 (ROR1), which in turn sustains a favorable balance between prosurvival PI3K-AKT

* Corresponding author. Fax: +81 52 744 2457.
E-mail address: tak@med.nagoya-u.ac.jp (T. Takahashi).

and pro-apoptotic p38 signaling [24]. However, TTF-1 expression is paradoxically known to be associated with favorable prognosis in lung adenocarcinoma patients [25], which can be explained, at least in part, by our recent discovery that myosin binding protein H (MYBPH) is directly transactivated by TTF-1 and inhibits RLC phosphorylation via direct interaction with ROCK1, which in turn reduces cell motility and metastasis [26].

Here, we report findings showing that MYBPH has another mode of inhibitory activity in regulation of NM IIA through direct binding to NMHC IIA, suggesting the existence of dual roles of MYBPH for firmly imposing inhibition of NM IIA assembly.

## 2. Materials and methods

### 2.1. Materials

Antibodies, reagents, PCR primers, siRNAs and recombinant proteins are summarized in Supplementary Tables 1–3.

### 2.2. Immunoprecipitation–Western blot analysis (IP–WB)

Cells ($2 \times 10^7$) were lysed with modified RIPA buffer containing 50 mM Tris–HCl (pH 8.0), 1 mM EDTA, 1% NP-40, 0.5% deoxycholate, 0.1% SDS, 20 mM β-glycerophosphate (pH 7.6), 50 mM NaF, 1 mM $Na_3VO_4$, and 150 mM NaCl, supplemented with Complete Protease Inhibitor Cocktail Tablets (Roche) and incubated with each antibody (5 μl) overnight at 4 °C, followed by addition of 80 μl of 50% protein G Sepharose (GE Healthcare) and subsequent incubation for 1 h. The immunoprecipitates were analyzed by Western blotting. In the input lane, a 1/100 amount of total cell lysate was applied to samples used in the immunoprecipitation experiments. In some experiments, NCI-H441 cells were treated with Y-27632 (5 μM) for 15 min before being harvested.

### 2.3. Negative staining and electron microscopy

The rod portions (0.66 μM) of GST-tagged NMHC IIA, and His-tagged MYBPH-wt or His-tagged MYBPHΔ-(1 + 2 + 3) were incubated in 100 μl of reaction mixture containing 10 mM Tris–HCl (pH 7.5), 0.1 mM EGTA, 1 mM EDTA, and 2.5 mM $MgCl_2$, supplemented with Complete Protease Inhibitor Cocktail Tablets in the presence of 150 mM NaCl overnight at 4 °C. For negative staining, aliquots of protein solution were placed on copper grids covered with carbon film and keep still for about 1 min to allow for adsorption of the molecules on the grids, after which the grids were washed with several drops of 2% uranyl acetate solution. Excess staining solution remaining on the grids was quickly absorbed with filter papers and dried. Images were obtained using a Hitachi H-7600 electron microscope (access 100 kV) onto film at a magnification of 50,000× and further processed with Adobe PHOTOSHOP software (Adobe Systems).

### 2.4. NMHC IIA sedimentation assay

The rod portions (0.66 μM) of GST-tagged NMHC IIA, and His-tagged MYBPH-wt or His-tagged MYBPHΔ-(1 + 2 + 3) were incubated in 100 μl of reaction mixture containing 10 mM Tris–HCl (pH 7.5), 0.1 mM EGTA, 1 mM EDTA, and 2.5 mM $MgCl_2$, supplemented with Complete Protease Inhibitor Cocktail Tablets in the presence of various concentrations of NaCl overnight at 4 °C. After ultracentrifugation at 186,000g for 60 min at 4 °C in a TLA 55 ultracentrifuge (Beckman), the supernatants were subjected to Western blot analysis. Western blot images of triplicate experiments were analyzed using ImageJ software with the input NMHC IIA utilized as a normalization control.

Other materials and methods are given in the Supplementary data.

## 3. Results and discussion

### 3.1. Combined treatment with siROCK1 and non-muscle myosin inhibitors inhibited cell motility increased by siMYBPH treatment

We recently showed that MYBPH inhibits ROCK1, and reduces cell motility and metastasis [26]. To better understand the functions of MYBPH in actomyosin organization, we treated MYBPH-silenced NCI-H441 cells with an NM II inhibitor blebbistatin [27]. Interestingly, increased cell motility of MYBPH-silenced NCI-H441 cells was partially suppressed by either siROCK1 or blebbistatin treatment, while combined treatment with those exhibited more profound effects than each alone (Fig. 1A). Another NM II inhibitor, 2,3-butanedione monoxime (BDM) [28], showed similar results (Fig. 1B). These findings suggest that MYBPH affects the assembly process of NM II not only at the ROCK1-mediated myosin regulatory light chain (RLC) phosphorylation step, but also via another as yet unidentified mechanism.

### 3.2. MYBPH binds to rod portion of NMHC IIA

It is well known that assembly of NMHC IIA is a crucial step toward actomyosin organization, because of its requirement for facilitating cell migration activity [4–8]. Therefore, we speculated that MYBPH somehow inhibits the NMHC IIA assembly process. To test this, we first examined the interaction between MYBPH and NMHC IIA using immunoprecipitation–Western blotting
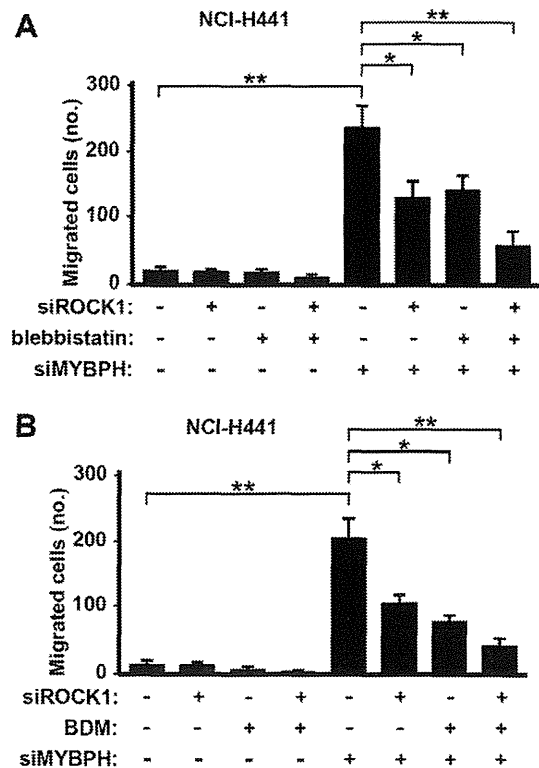


Fig. 1. Combined treatment with both siROCK1 and non-muscle myosin inhibitors inhibits increased cell motility induced by siMYBPH. (A) Motility assay in NCI-H441 cells co-treated with si-ROCK1 and the non-muscle myosin-specific inhibitor blebbistatin [27], as compared to each alone. Bars, mean ± SD; *P < 0.05; **P < 0.005. (B) Motility assay in NCI-H441 cells co-treated with si-ROCK1 and pan-myosin inhibitor 2,3-butanedione monoxime (BDM) [28], as compared to each alone. Bars, mean ± SD; *P < 0.05; **P < 0.001.
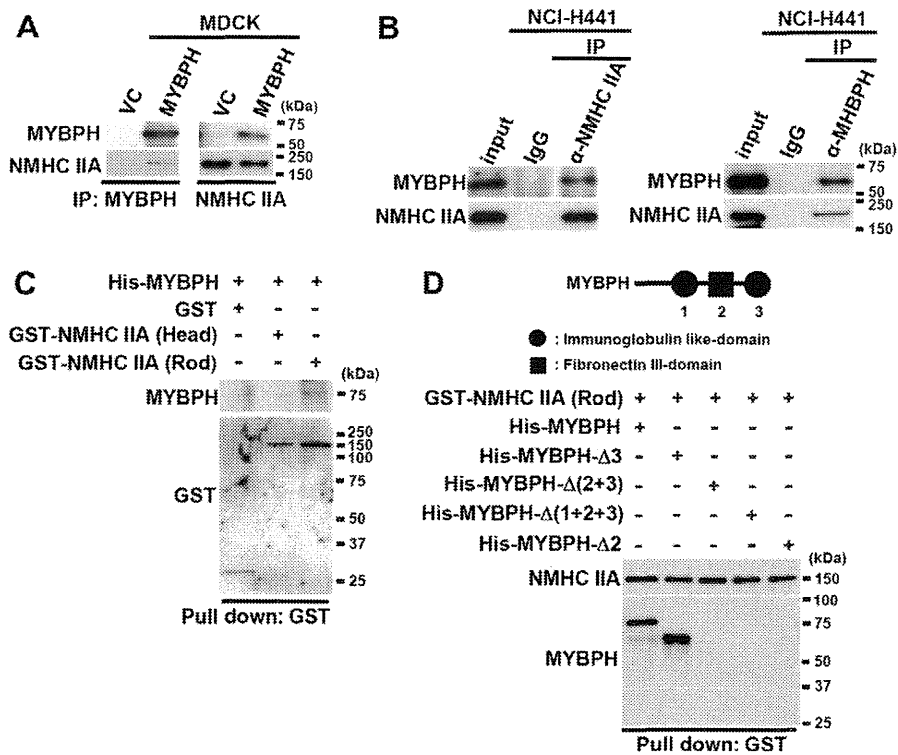
Fig. 2. MYBPH binds to the rod portion of NMHC IIA. (A) Immunoprecipitation–Western blot (IP–WB) analysis in MDCK cells expressing exogenous MYBPH. VC, vector control. (B) Top panel: findings of IP–WB analysis using anti-NMHC IIA antibody in H441 cells expressing endogenous MYBPH. Bottom panel: IP–WB analysis using anti-MYBPH antibody. (C) In vitro protein–protein binding assay of purified proteins of MYBPH and rod portion of NMHC IIA. The binding assay was performed as previously described [26]. (D) Top panel: schematic representation of domain organization of MYBPH. Bottom panel: in vitro protein–protein binding assay between MYBPH and NMHC IIA.

(IP–WB) analysis, and found that MYBPH bound to NMHC IIA in MYBPH-over-expressing MDCK cells, as well as NCI-H441 cells that endogenously express MYBPH (Fig. 2A and B). To assess the specificity of this interaction, an in vitro protein–protein binding assay using recombinant proteins was performed, which clearly demonstrated that MYBPH directly interacts with the rod portion of NMHC IIA (Fig. 2C). We also investigated which domain of MYBPH is important for its binding to the rod portion of NMHC IIA using various deletion mutants. The fibronectin type III domain of MYBPH was shown to be required for MYBPH binding to NMHC IIA (Fig. 2D), which appears to be in agreement with its structural resemblance to MYBPC [29].

### 3.3. MYBPH inhibits NMHC IIA assembly

To examine the effect of MYBPH on NMHC IIA assembly, we performed electron microscopy analysis, and visualized the assembled structures of NMHC IIA rod fragments in the presence of either wild-type MYBPH or an MYBPH-Δ (1 + 2 + 3) mutant. The rod-portion of NMHC IIA formed long and well-ordered paracrystal structures in the presence of an MYBPH-Δ (1 + 2 + 3) mutant, which lacks a capacity to bind to NMHC IIA, whereas those paracrystals were poorly developed in the presence of wild-type MYBPH. (Fig. 3A). To confirm that MYBPH inhibits NMHC IIA assembly, we also performed sedimentation assays under various salt concentrations using the rod portion of NMHC IIA, and either wild-type MYBPH or the MYBPH-Δ (1 + 2 + 3) mutant. A greater amount of unassembled NMHC IIA was observed in the presence of the wild-type than with the mutant (Fig. 3B). These results indicated that MYBPH inhibited the assembly of NMHC IIA through direct interaction. Phosphorylation of NMHC IIA on its tail region has been shown to cause NMHC IIA disassembly [5], suggesting its potential involvement. However, MYBPH did not appear to be

involved in that process, since the phosphorylation status of NMHC IIA was not affected by knockdown of MYBPH in NCI-H441 cells or its over-expression in MDCK cells (Fig. 3C).

### 3.4. MYBPH has higher affinity to assembly-competent NMHC IIA monomer

Upon RLC phosphorylation, assembly-incompetent NM IIA unfolds and changes to an assembly-competent form, which is a prerequisite prior to forming bipolar NM IIA filaments and consequential linking of actin filaments [4,5]. IP–WB analysis showed reduced interaction between MYBPH and NMHC IIA in NCI-H441 cells treated with the ROCK inhibitor Y-27323, which impairs transition of NM IIA from an assembly-incompetent to -competent state (Fig. 3D), suggesting that MYBPH has a higher affinity to assembly-competent NM IIA. In order to examine whether MYBPH preferentially interact with the monomer form of NMHC IIA and inhibit its assembly, we performed in vitro binding assays using purified proteins of MYBPH and the rod portion of NMHC IIA under low and high salt concentration conditions, in which NMHC IIA is presumed to be in a predominantly dimer and monomer state, respectively. Our results demonstrated that MYBPH binds to NMHC IIA more efficiently in high as compared to low salt concentrations (Fig. 3E). Thus, MYBPH has a higher affinity to the assembly-competent and monomer forms of NMHC IIA.

### 3.5. Organization of peripheral actomyosin bundles induced by MYBPH knockdown counteracted by simultaneous treatment with non-muscle myosin inhibitors

MYBPH knockdown induces co-localization of NMHC IIA with the peripheral actin bundles, forming peripheral actomyosin bundles in NCI-H441 cells [26]. The present findings showed that
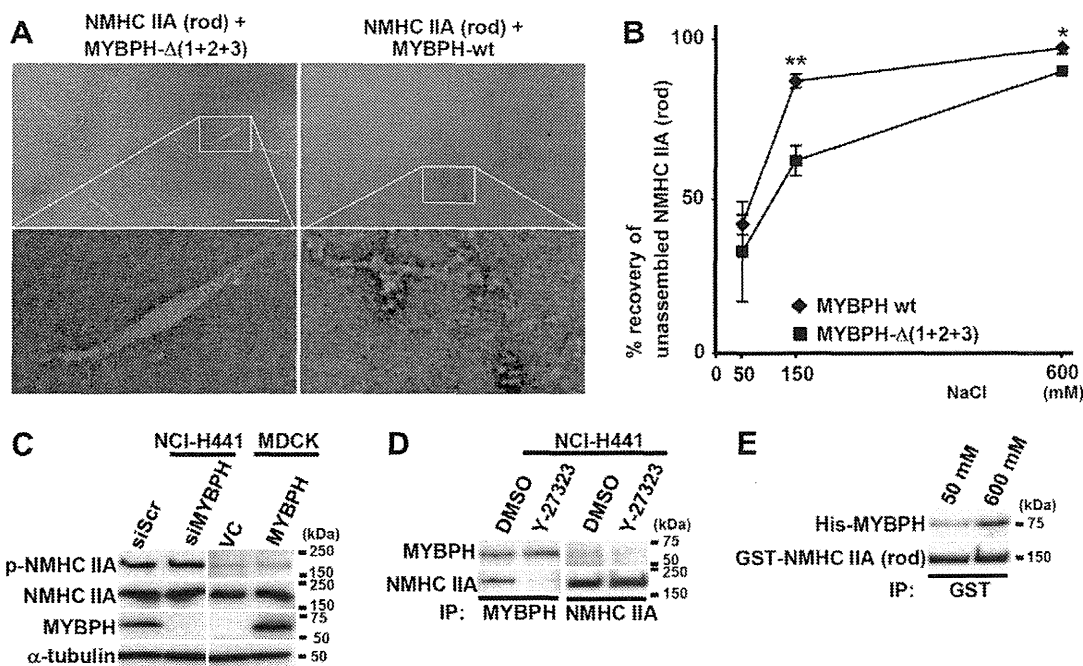
Fig. 3. MYBPH inhibits NMHC IIA assembly and has higher affinity to assembly-competent NMHC IIA monomer. (A) Electron microscopy analysis. Bar indicates 200 nm. (B) Sedimentation assay using rod portion of NMHC IIA in presence of wt-MYBPH. Bars, mean ± SD; *P < 0.01; **P < 0.005. (C) Western blot analysis in HCl-H441 cells knocked down for MYBPH or MDCK cells overexpressing MYBPH. (D) IP–WB analysis in NCl-H441 cells treated with ROCK inhibitor Y-27632. (E) In vitro protein–protein binding assay in various salt conditions.

siMYBPH-induced formation of the peripheral actomyosin bundles was significantly counteracted by simultaneous treatment with blebbistatin or BDM (Fig. 4A, high power field; Supplementary Fig. 1, low power field). Using a three-dimensional Matrigel invasion assay, we previously showed that ROCK1 inhibition clearly cancelled siMYBPH-induced single cell migration [26]. To examine whether NMHC IIA inhibition similarly affects siMYBPH-induced single cell migration, we treated NCl-H441 cells with siMYBPH and/or blebbistatin. We found that while siMYBPH induced single cell migration in accordance with our previous report, siMYBPH-treated NCl-H441 cells did not revert to the collective migratory phenotype in the presence of blebbistatin (Fig. 4B). In addition, it has been proposed that collective cell migration requires decreased ROCK1-driven actomyosin activity at the cell–cell junction in conjunction with sustainment of CDC42-dependent actomyosin activity around the outside surface of cell clusters [30,31]. Therefore, it is possible that cancelation of siMYBPH-induced single cell migration by the ROCK1 inhibitor alone may have been caused by distinct actomyosin inhibition patterns between ROCK1 inhibitor- and blebbistatin-treated cells, the latter of which inhibits actomyosin in both the cell–cell junction and on the cell cluster surface.

### 3.6. MYBPH may negatively regulate actomyosin organization at 2 distinct steps

We previously reported that MYBPH is a transcriptional target of the TTF-1 lineage-survival oncogene and plays a crucial role in inhibition of cancer cell motility, invasion, and metastasis [26]. While it was shown to be imposed through inhibition of RLC phosphorylation via physical interaction with and inhibition of ROCK1, the present findings further demonstrate that MYBPH has an additional binding molecule, namely NMHC IIA. MYBPH binds to the rod portion of NMHC IIA and inhibits its assembly, which is thought to take place following acquisition of assembly-competence conferred through RLC phosphorylation by ROCK1 [9,10]. This implies that MYBPH inhibits 2 independent components of

NM IIA, i.e., RLC and NMHC IIA, and thereby negatively regulates actomyosin organization at 2 distinct steps (Fig. 4C). Along this line, the additive effects of combined treatment with siROCK1 and blebbistatin on siMYBPH-induced increased motility may result from residual basal level competence, as there is compelling evidence showing that the transition between assembly-incompetent and -competent NMHC state is in equilibrium at a physiological ionic level (150 mM NaCl, pH 7.0) even in the absence of RLC [32]. Thus, this dual step inhibition of NM IIA assembly by MYBPH may play a role as a possible mechanism for imposing firmer inhibition.

### 3.7. Physiological and pathological implication of MYBPH inhibition at NMHC IIA assembly step

The NM IIA-attributed functions for regulating actomyosin organization are thought to be involved in development and progression of various types of cancer [6–8], while the involvement of RLC phosphorylation and RLC kinases such as ROCK1 in cancer progression is well established [11–14]. Nevertheless, to date very few regulators of NMHC IIA have been reported. S100A4, also called MTS1, mediates NMHC IIA disassembly via direct interaction, while casein kinase II (CK II) also disassembles NMHC IIA through phosphorylation of NMHC IIA on its tail region [15,33]. The present results showed that MYBPH binding to NMHC IIA does not affect this phosphorylation. Taken together, our findings add MYBPH to the very short list of physiological inhibitors of NMHC IIA assembly.

In addition to its effects on cancer progression, NMHC IIA has been found to play important roles in a wide range of disease states such as MYH9-related disorders, which exhibit a combination of different phenotypic features including large platelets and thrombocytopenia [34,35]. Defects in NMHC IIA assembly due to mutations in the rod portion of NMHC IIA are thought to be major causes of MYH9-related disorders. Thus, we consider it interesting